University of Glasgow | School of Physics & Astronomy

Astronomy 345: High Energy Astrophysics I

Session 2021-22

11 Lectures, starting September 2021

Lecturer: Prof. Eduard Kontar

Kelvin Building, room 615, extension x2499

Email: Eduard (at) astro.gla.ac.uk

Lecture notes and example problems - https://moodle2.gla.ac.uk

last update: September 30, 2021

Contents

1 Introduction to High Energy Astrophysics

LECTURE OUTLINE

- Intended learning outcomes
- Recommended literature
- History of X-rays
- Classification and key terminology

1.1 Course aims

- To introduce students to the **physical processes responsible for X-Ray production**, as a basis for the applications discussed in X-Ray Astrophysics II
- To introduce students to the concept of a **reaction cross-section**, and to explain how to calculate **X-Ray emission rates and spectra** from specified source conditions

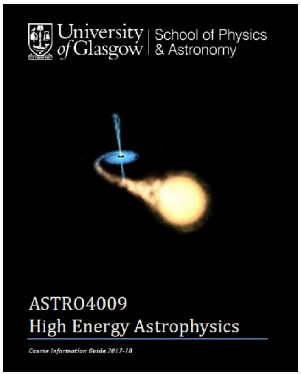

Further details are also available in Course Handbook

1.2 Recommended literature and useful resources:

These lecture notes are following the material from:

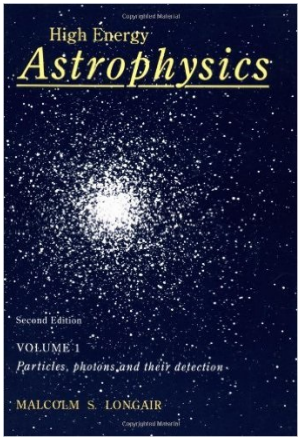

Malcolm S. Longair, *High energy astrophysics, volume 1 & 2*, High energy astrophysics, 1992, UofG Library link or e.g. Amazon

1.3 A Brief History of X-rays

Wilhelm Roentgen

- **Oct 1895** Wilhelm Roentgen begins to study Cathode Rays (discovered decades earlier)
- **8 Nov 1895** Roentgen notices glowing fluorescent screen some distance away from cathode ray tube - realises he has discovered a new phenomenon: **X-rays**
- **22 Dec 1895** Roentgen photographs his wife's hand - The first X-Ray Picture

First X-ray Picture

Print of Wilhelm Rontgen's first X-ray, of his wife's hand, taken on 22 December 1895 and presented to Ludwig Zehnder of the Physik Institut, University of Freiburg, on 1 January 1896

X-ray timeline:

- **28 Dec 1895** Discovery announced at Wurzburg Physico-Medical Society
- **4 Jan 1896** Discovery announced at Berlin Physical Society
- **Jan 1896** Discovery published in newspapers around the world
- **2 Mar 1896** Henri Becquerel discovers natural radioactivity of *Uranium*

1.4 From the past till now

- **1901** First ever Nobel Prize in Physics awarded to Roentgen
- **1903** Third Nobel Prize in Physics awarded to Becquerel, Pierre and Marie Curie
- **...**
- **1999** Launch of CHANDRA and XMM X-ray satellites
- **2002** Launch of RHESSI X-ray and gamma-ray satellite
- **2008** Launch of Fermi X-ray and gamma-ray satellite
- **2012** Launch of NuSTAR X-ray satellite by NASA
- **February 2020** Solar Orbiter with STIX X-ray imager

1.5 X-ray Region of Electromagnetic Spectrum

Wavelength λ:

$$0.01\text{nm} \lesssim \lambda \lesssim 10\text{nm}$$

$$0.1 \quad \text{Å} \lesssim \lambda \lesssim 100\text{Å}$$

where $1\text{nm} = 10^{-9}$ m, $1\text{Å} = 10^{-10}$ m.

Corresponding **photon energy**:

$$E = h\nu = \frac{hc}{\lambda} = \frac{6.63 \times 10^{-34} \times 3 \times 10^{8}}{1.6 \times 10^{-19}\lambda[\text{m}]}[\text{eV}] = \frac{12.4}{\lambda[\text{Å}]}[\text{keV}]$$

where $1\text{ eV} = 1.602 \times 10^{-19}$ J.

$1\text{ keV} = 10^{3}\text{ eV}, \quad 1\text{ MeV} = 10^{6}\text{ eV}, \quad 1\text{ GeV} = 10^{9}\text{ eV}, \quad 1\text{ TeV} = 10^{12}\text{ eV}$

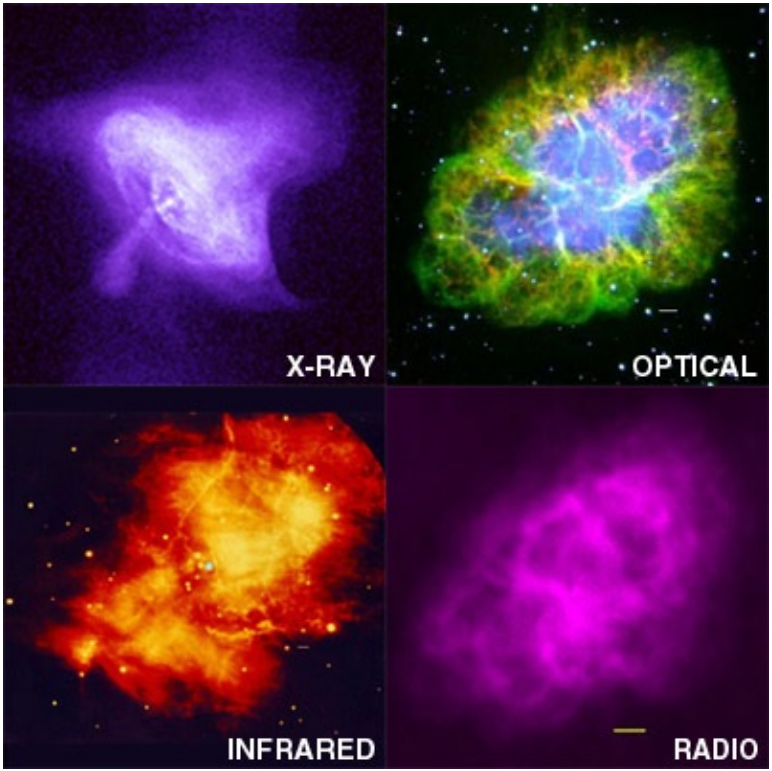

Figure 1.1: *Image of Crab nebula at different wavelengths/frequencies* *Chandra, Harvard*

1.6 Classification/terminology

	Energy range	Wavelength range
Soft X-rays	$0.1 - 1$ keV	$\sim 100 - 10$Å
Classical X-rays	$1 - 10$ keV	$\sim 10 - 1$Å
Hard X-rays	$10 - 100$ keV	$\sim 1 - 0.1$Å
Gamma-rays (γ-rays)	$\gtrsim 0.1$ MeV	$\lesssim 0.1$Å

Note that the classification/terminology is somewhat different in various areas of Astrophysics.

Energy $\Longleftrightarrow$ Temperature:

$$E \simeq k_B T \quad \Longrightarrow \quad 1\text{keV} \simeq 10^7\text{K}$$

where $k_B = 1.38 \times 10^{-23}$ J/K Boltzmann constant.

Hence to produce X-rays we need very high temperatures!

1.7 X-ray and atmosphere

Only a few windows in the E-M spectrum exist for ground-based observations: optical and radio (see Figure 1.2).

Space-based observations opened up rest of E-M Spectrum.

Classical X-rays:

- These are readily absorbed (photoelectric absorption) by gases, liquids and solids
- Unable to penetrate the Earth's atmosphere
- Observations must be made at altitudes above 100 km using rockets or satellites

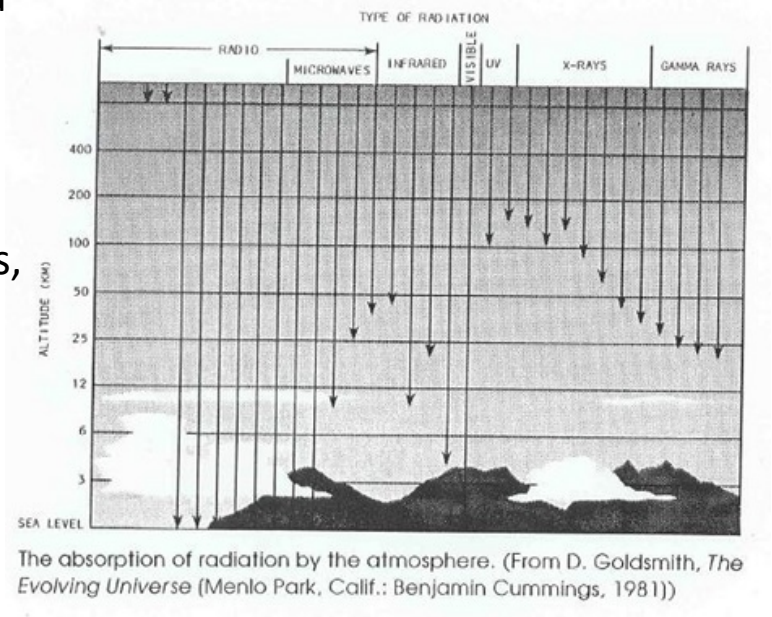

Figure 1.2: *X-ray and gamma-ray penetration via atmosphere*

Hard X-rays:

• More penetrating than classical X-rays. Observations can be made from e.g. balloon platforms at ~ 30 km altitude

Soft X-rays:

• Much weaker flux than classical or hard X-rays. Strongly attenuated by interstellar gas in the galaxy

1.8 Useful wavelength range for Astronomy

Useful range for obtaining **astronomical information:**

$$10^{-21}\text{m} \lesssim \lambda \lesssim 10^{4}\text{m}$$

- For $\lambda \lesssim 10^{-21}$m (Energy $\gtrsim 10^{15}$ eV), γ-rays readily destroyed by collisions with CMBR photons, producing electron-positron pairs
- For $\lambda \gtrsim 10^{4}$m , radio waves are absorbed by solar wind plasma (cut-off frequency near Earth ~ 20 kHz) . Earth ionosphere produces cut-off near 10 MHz

1.9 Luminosity of a bright X-ray star

Scorpius X-1 delivers roughly 10^6 m^{-2} s^{-1} **classical X-ray** photons to the Earth.

Since the *typical energy of classical X-ray photon*

$$E_{X1} = 5\text{keV} = 8 \times 10^{-16}\text{J}\,,$$

the energy flux is

$$F_{X1} = 8 \times 10^{-16} \times 10^6 = 8 \times 10^{-10}\text{W/m}^{\,2}$$

Given the distance $D = 2800$ pc [recall 1 pc=3.1×10^{16} m]

Luminocity: $L_{X1} = 4\pi D^2 F = 4\pi(9 \times 10^{19})^2 \times 8 \times 10^{-10}\text{W} \simeq 8 \times 10^{31}\text{W}$

hence, recalling that $L_\odot \simeq 4 \times 10^{26}$ W

$$L_{X1} \simeq 10^5 L_\odot$$

Bright X-ray sources in our galaxy similar to Sco X-1 include:

- **compact binaries**
- **supernova remnants**

But these are sparse. The Galaxy contains only 100 X-ray sources with $L > 10^{28}$ W.

Taking as a typical luminosity of a bright X-ray source $L \sim 10^{31}$ W, the total X-ray luminosity for the galaxy

$$L_X \sim 10^{33}\text{W}$$

Let us compare this with the total bolometric luminosity of stars

$$L_{bol} \sim 10^{11}\text{stars} \times 4 \times 10^{26}\text{W} \sim 4 \times 10^{37}\text{W}$$

So X-ray emission is only~ 0.01 % of the bolometric luminosity of the Milky Way - i.e. **we are not (any more) an active galaxy**

2 Observing X-rays in Astrophysics

LECTURE OUTLINE

- Past, present and future high energy observations
- Astrophysical objects at high energies
- X-ray and gamma ray observation techniques: grazing incidence optics, collimators
- X-ray spectroscopy

2.1 X-ray Astronomy observations from Space

Rocket experiments started with captured German V2 rockets. (Although the flight lasted for only a few minutes)

- **1948** Solar X-rays detected (from the **solar corona**)
- **1962** Bright X-ray source discovered in Scorpius; star denoted Sco X-1
- **1963** Isotropic X-ray background discovered; Extragalactic Sources; X-ray source detected in Crab Nebula
- **1966** X-ray galaxies identified

2.2 Satellite Missions

Since 1970 till present day large number of satellites launched to observe various astrophysical objects in X-rays e.g. **ROSAT, Yohkoh, SoHo, XMM, Chandra, RHESSI,...**

Main observational results:

- Huge numbers of sources detected (e.g. 60000 by ROSAT; > 10 times more by XMM, Chandra)

- Many X-ray binaries identified (e.g. Cygnus X-1, black hole candidate)

- Detailed observations of solar flares, pulsars, quasars, galaxy clusters, supernova, galaxies, moon, comets...

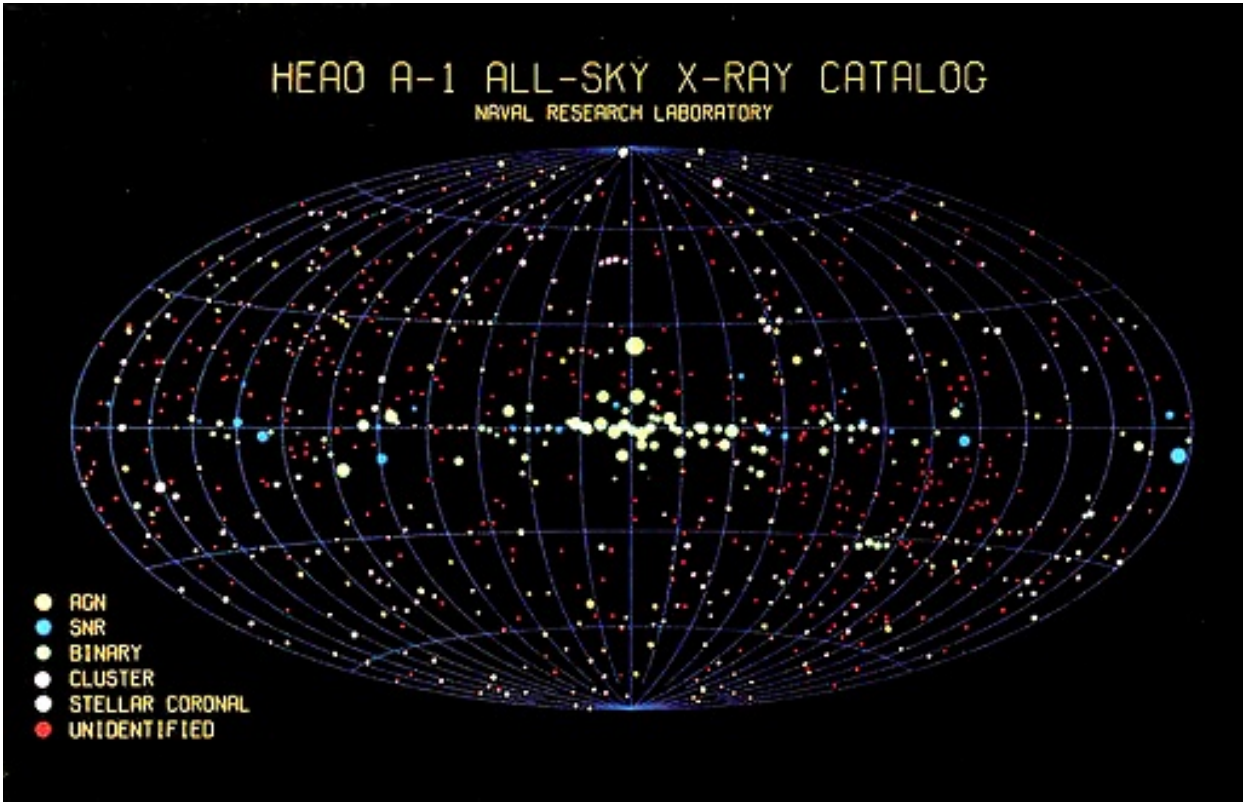

Figure 2.1: *ROSAT X-ray bright sources see ROSAT webpage*

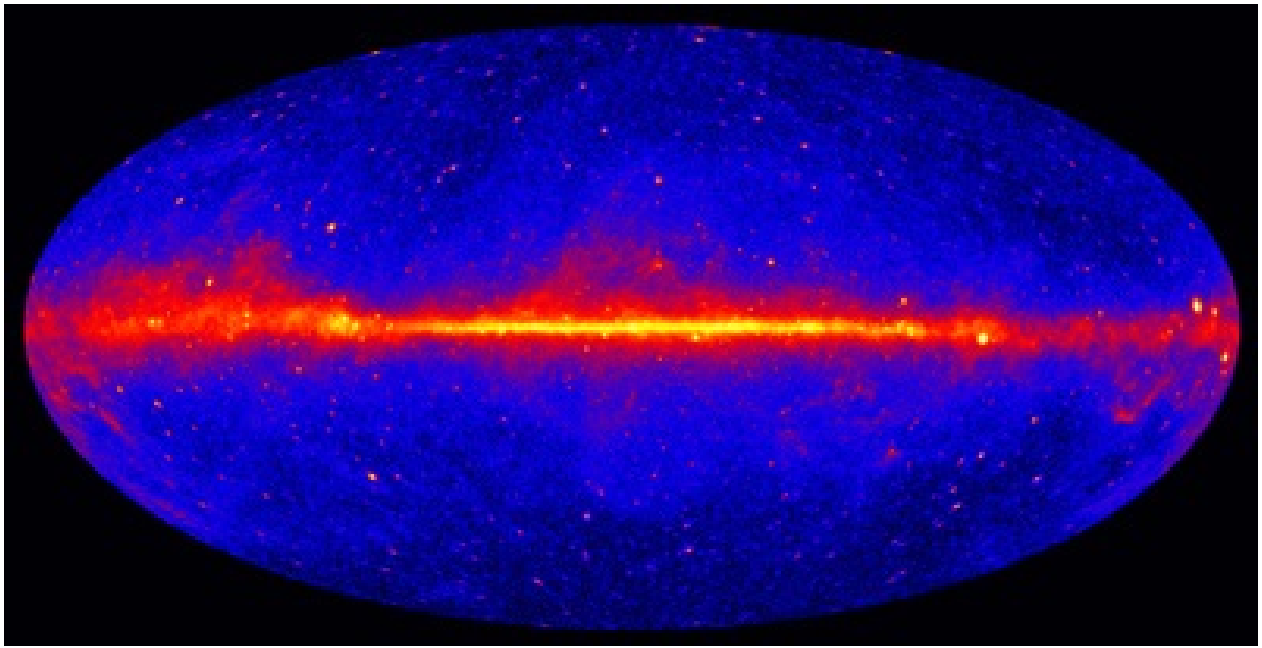

Figure 2.2: *All sky map of gamma-ray counts above 1 GeV from NASA Fermi data*

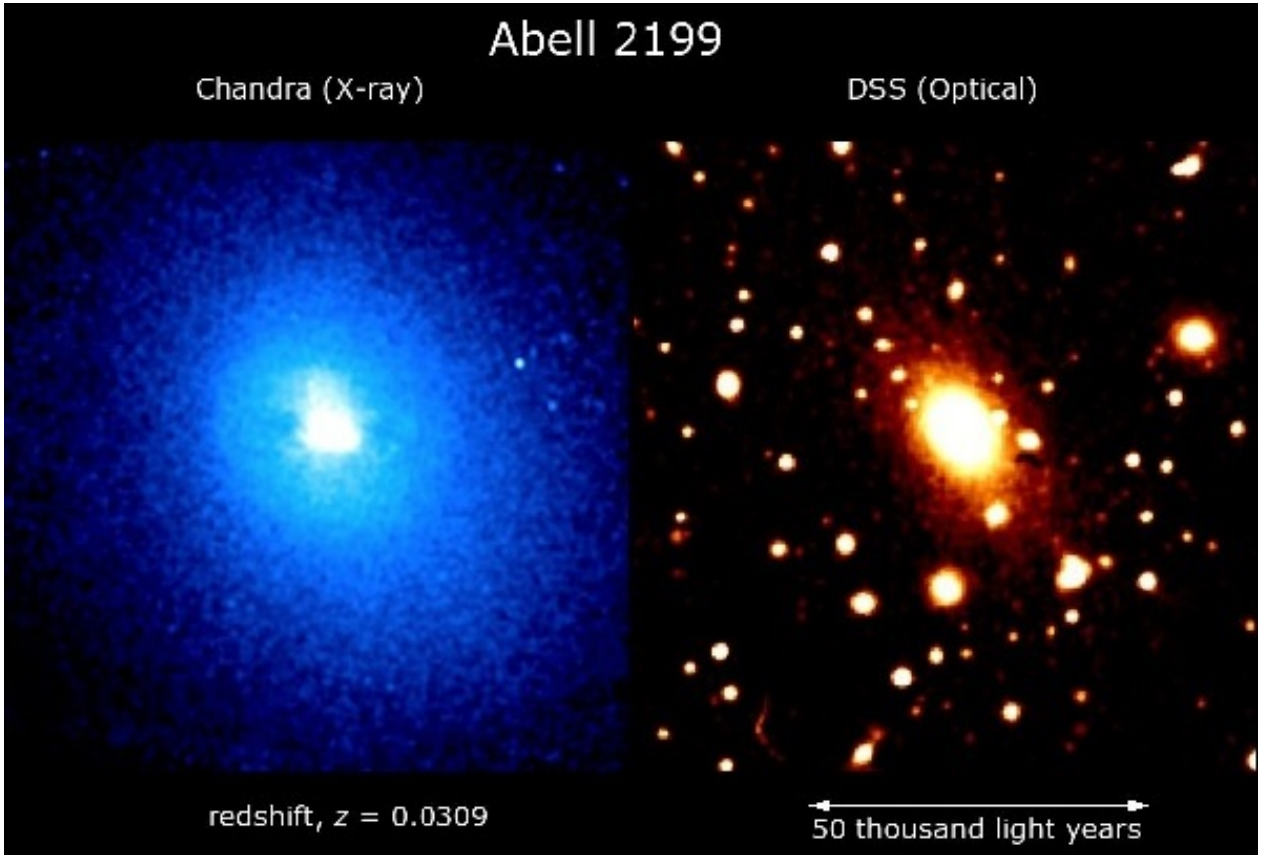

Figure 2.3: *Abell galaxy cluster by Chandra X-ray observatory*

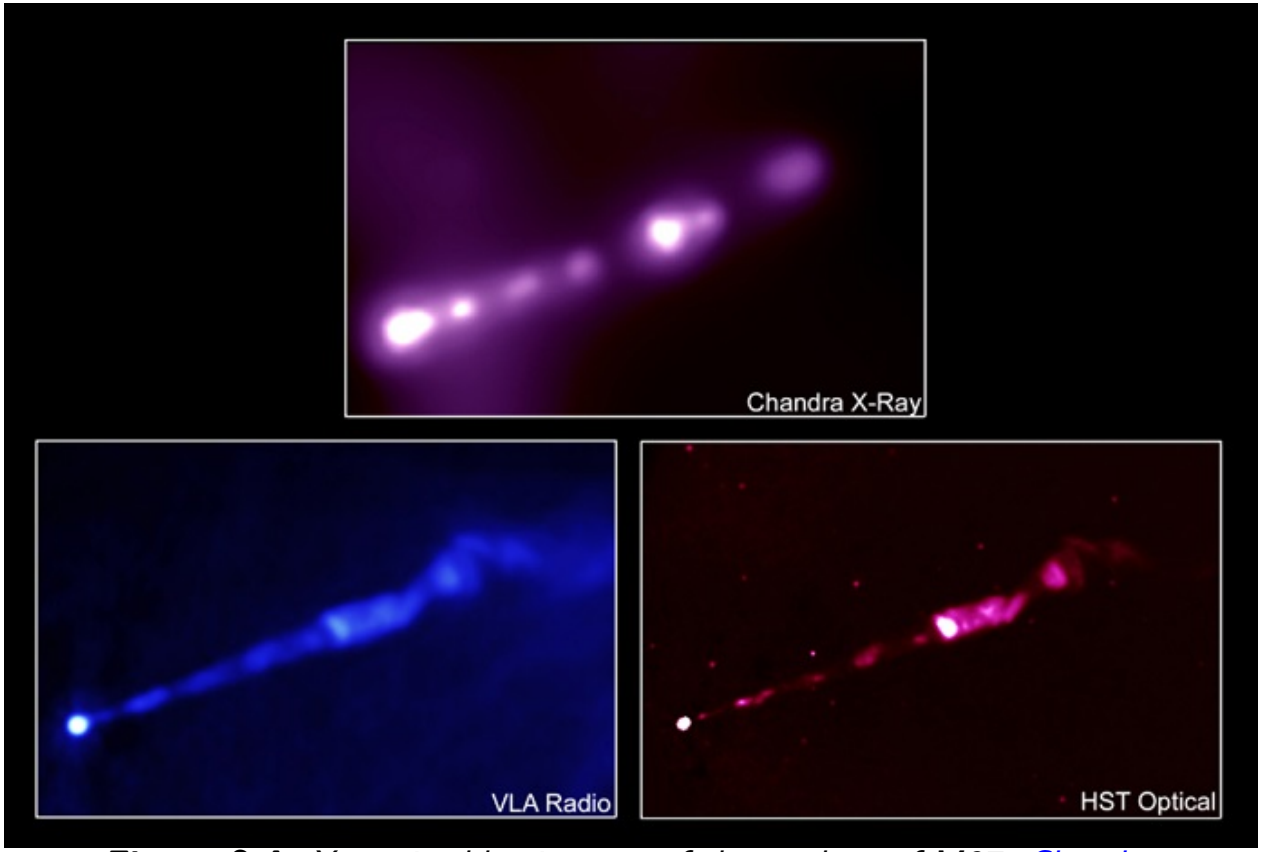

Figure 2.4: *X-ray jet blasting out of the nucleus of M87* *Chandra*

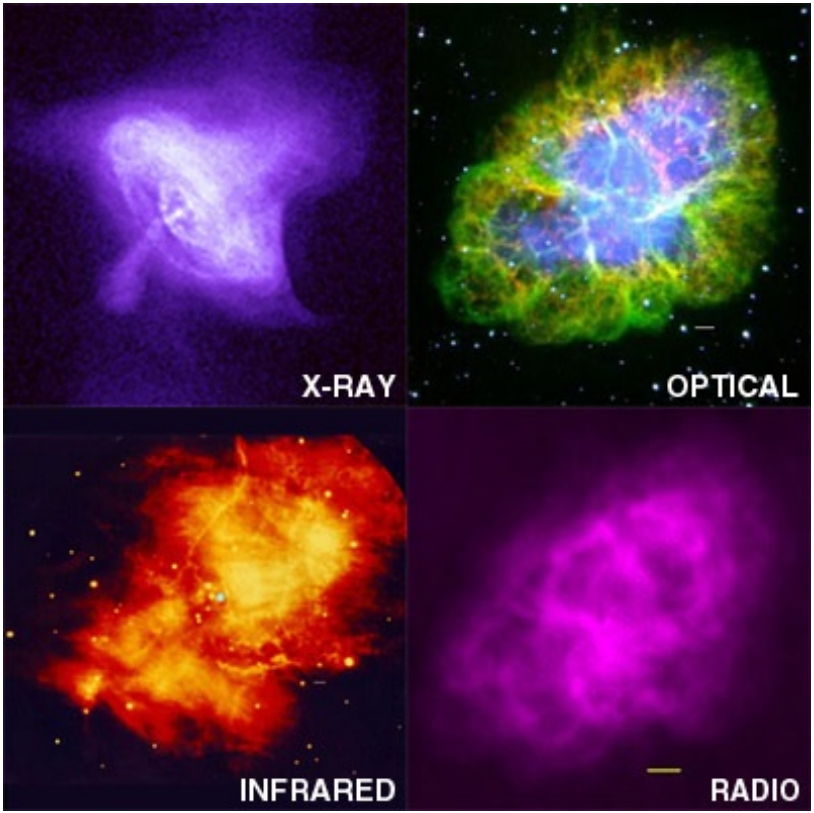

Figure 2.5: *X-ray image of Crab nebula from Chandra, Harvard*

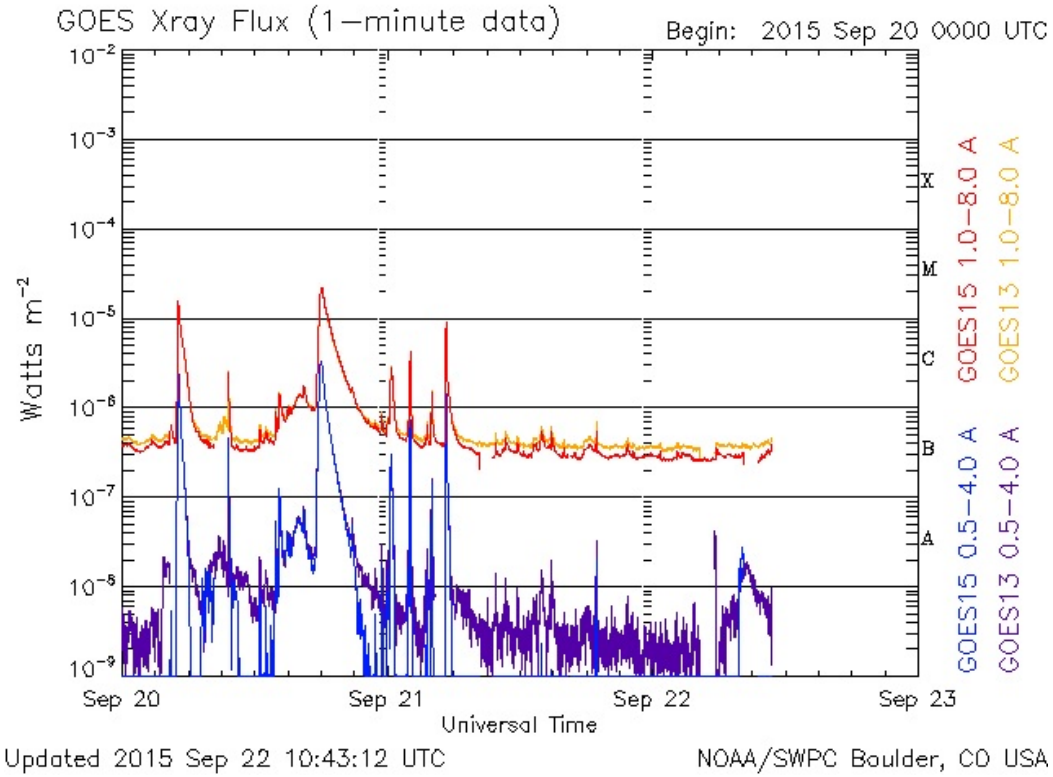

Figure 2.6: *GOES soft X-ray flux from the Sun. [Image from NOAA Space Weather Prediction Center] REAL-TIME soft X-rays from the Sun*

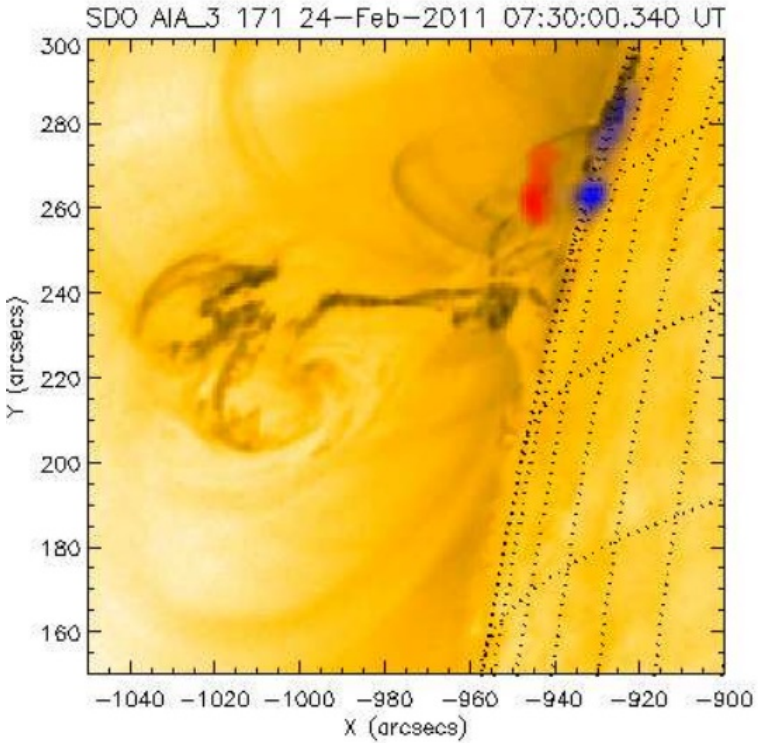

Figure 2.7: *SDO and RHESSI observations of a solar flare: $\sim 10^6$ K corona plasma (yellow), 10 keV X-ray (red), > 30 keV X-rays (blue) from Astronomy & Astrophysics*

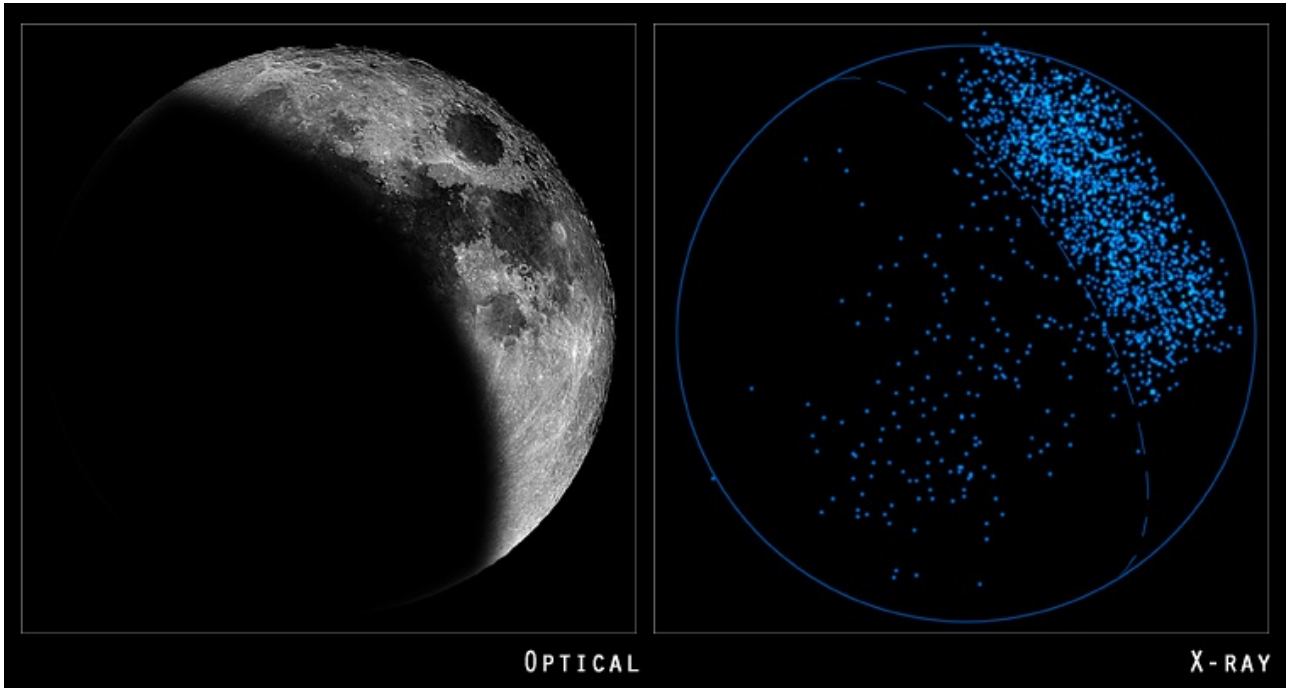

Figure 2.8: *X-rays are produced by fluorescence when solar X-rays bombard Moon Chandra, Harvard*

2.3 Athena (due for launch in early 2030s)

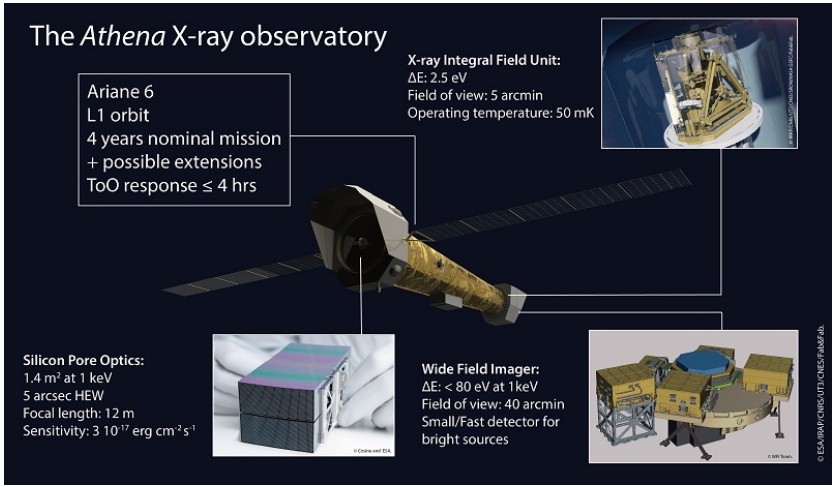

Figure 2.9: *Athena mission, Athena webpage*

Athena (Advanced Telescope for High ENergy Astrophysics) is the X-ray observatory mission selected by ESA to address the Hot and Energetic Universe scientific theme.

Athena (Fig. 2.9) will consist of a single large-aperture **grazing-incidence** X-ray telescope, utilizing a novel technology (High-performance Si pore optics), with 12 m focal length and 5 arcsec HEW on-axis angular resolution.

2.4 Grazing Incidence Optics

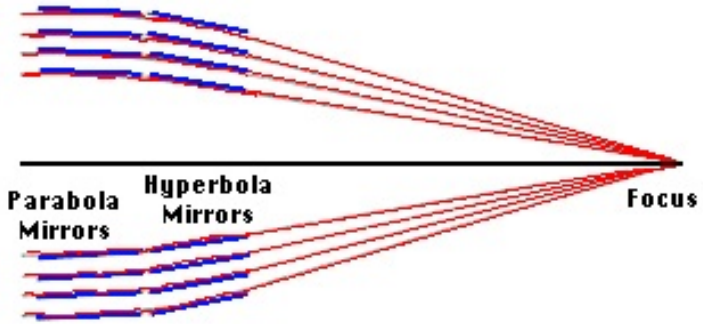

Figure 2.10: *Grazing Incidence Optics*

For low energy photons $E < 10$ keV, **Grazing Incidence Optics** can be used. Series of nested surfaces of highly conducting material (e.g. Cu), so that X-ray photons reflected for large incidence angles **Grazing Incidence** (Fig. 2.10).

Limited angular resolution (but improving all the time, e.g. XMM Newton: 5 arcsec resolution (Fig 2.11); also X-ray spectra)

Works OK but only up to a few tens of keV.

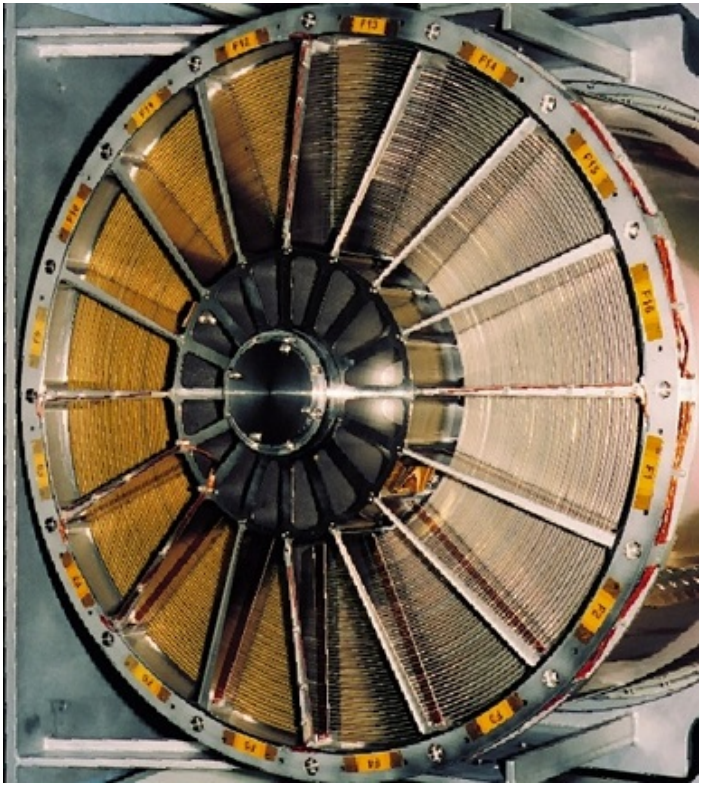

Figure 2.11: *XMM Newton X-ray optics.*

2.5 Mechanical collimators

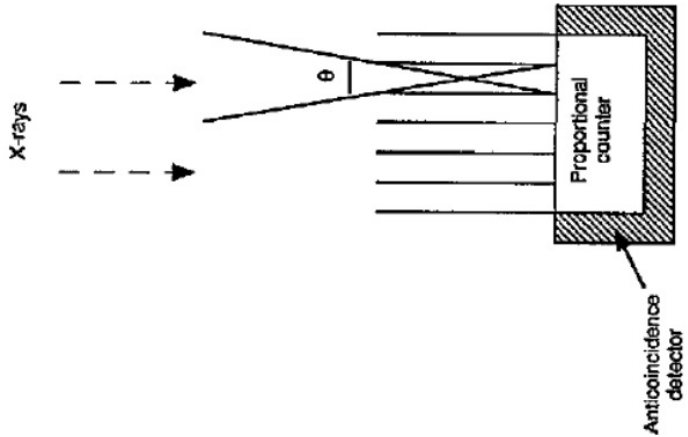

Figure 2.12: *Mechanical collimator*

Mechanical collimators block X-rays from unwanted parts of the sky.

The layout of a simple X-ray telescope of the type flown on the UHURU and Ariel-V satellite is shown in Fig 2.12.

Angle θ gives angular resolution of such telescope.

Proportional counters are used as detectors (see Figure 2.12) shielded by **anti-coincidence detectors**.

2.6 Rotating modulating collimators

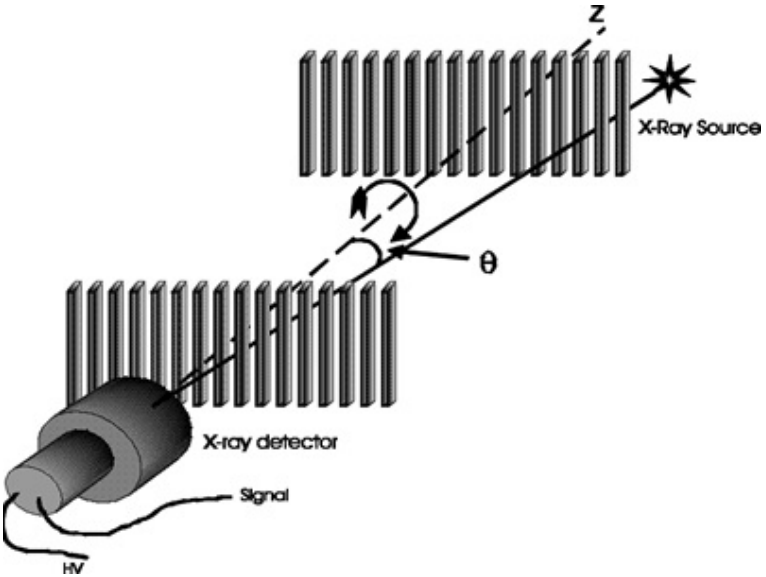

Figure 2.13: *Rotating modulating collimator. Two grids modulate incoming photon flux.*

For example, Ramaty High Energy Solar Spectroscopic Imager (RHESSI) satellite detectors look at the source through a pair of grids called **Rotating Modulating Collimator (RMC)**.

As spacecraft spins about once every ~ 4 sec, artificial modulation of incoming X-ray flux appears in the detectors.

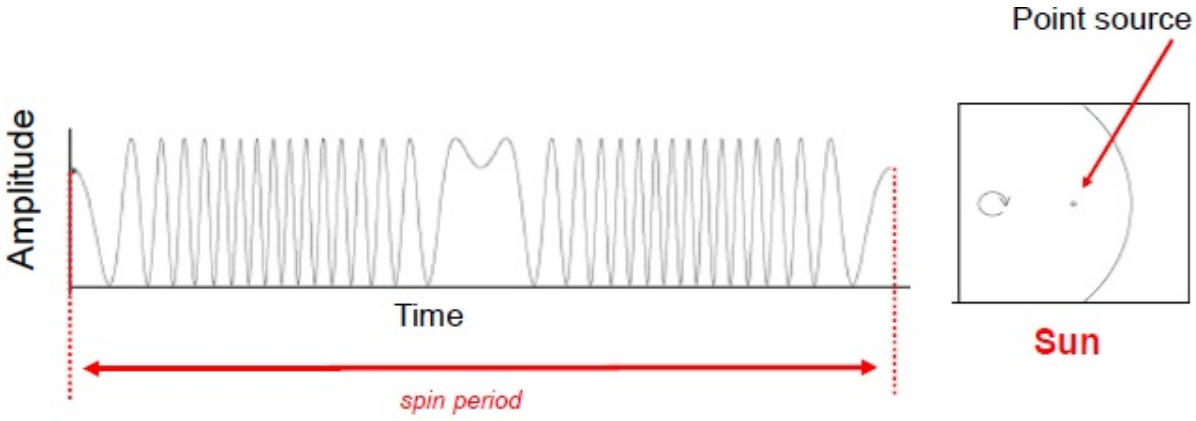

Figure 2.14: *Modulation of incoming X-ray flux from a point source using Rotating Modulating Collimator (see Fig 2.13).*

2.7 RHESSI

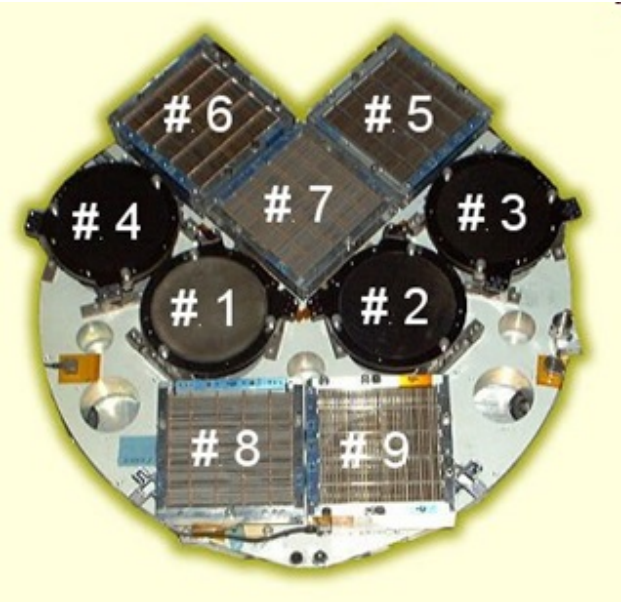

Figure 2.15: *RHESSI grids see Hurford et al, 2002 for details. Modulation using RMC see Figure 2.13.*

RHESSI is designed to investigate particle acceleration and energy release in solar flares through imaging and spectroscopy of hard X-ray and gamma-rays in the range from 3 keV up to 17 MeV (Lin et al 2002).

RHESSI has 9 Ge detectors (see Fig 2.16) and rotating modulating collimators allowing angular resolution down to 2.3 arcsec.

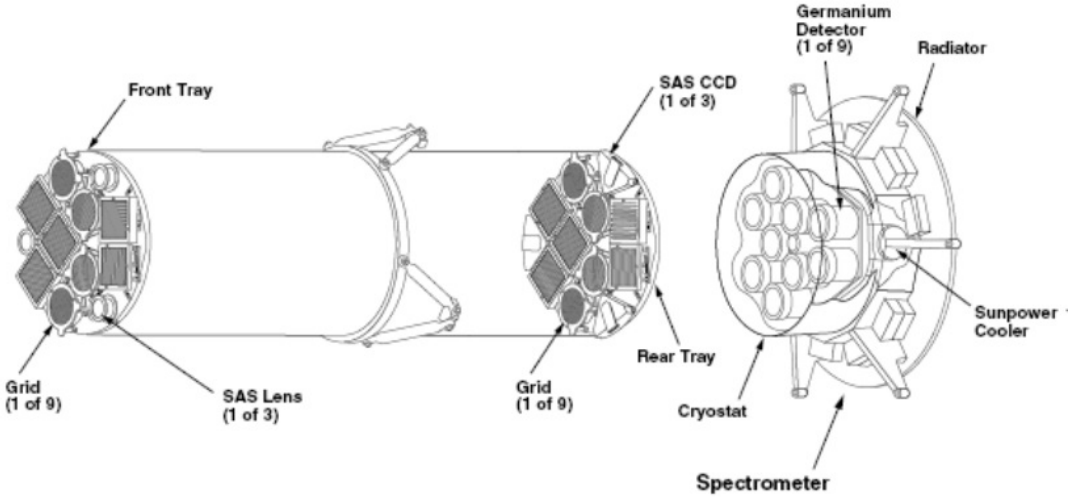

Figure 2.16: *RHESSI has 9 RMCs for 9 detectors Slats/Slits spacing growing with detector (RMC) number angular resolution from 2.3 arcsec (RMC #1) to 180 arcsec (RMC #9)*

2.8 Germanium detectors X-ray spectroscopy

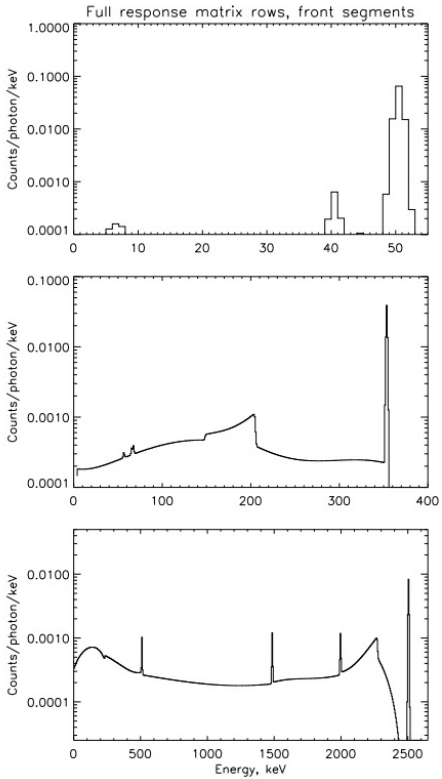

Hard X-ray photon interacting in the cooled semiconductor crystal (e.g. Germanium) releases one or more energetic electrons, which lose energy by creating free electron-hole pairs. The electrons and holes pulled to each electrode by high voltage, creating a **current pulse proportional to the photon energy**. The current pulse is amplified and digitized by suitable electronics.

For example, **RHESSI** spacecraft observes solar photons from 3 keV to 17 MeV using cooled coaxial germanium detectors.

Figure 2.17: *RHESSI response matrices. Sample responses at 50, 350 and 2500 keV Smith et al, 2002 for details. Modulation using RMC see Figure 2.13.*

3 X-ray emission mechanisms, Black-body emission

LECTURE OUTLINE

- Introduction into high energy emission mechanisms
- Thermal radiation, optical depth, bremsstrahlung, inverse Compton scattering, synchrotron radiation
- Black-body emission, X-ray spectrum

3.1 Thermal Mechanisms

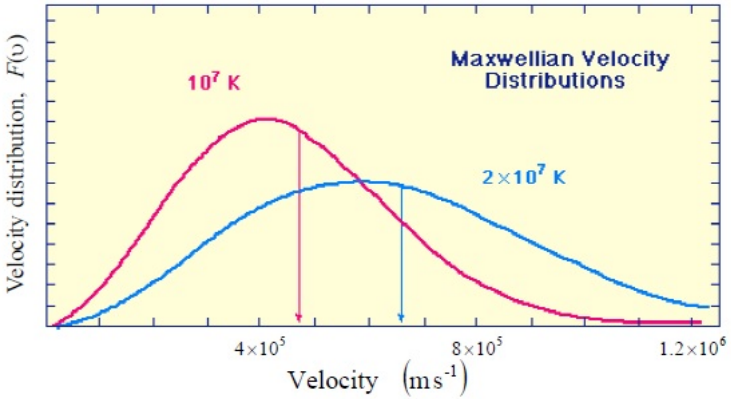

Figure 3.1: *Maxwellian velocity distribution*

Hot gas (plasma) in **thermal equilibrium** has a Maxwellian distribution of velocities:

$$f(v) \sim v^2 \exp\left(-\frac{mv^2}{2k_B T}\right)$$

For X-rays, say 1 keV we have

$$T \sim 10^7 \text{K}$$

We can have 2 regimes: **optically thick**, **optically thin**.

3.2 Optical depth

Optical depth, τ gives a measure of how opaque a medium is to radiation passing through it.

Recall definition of optical depth from Astronomy 2. The intensity[1] of radiation

$$I(\tau) = I_0 \exp(-\tau), \qquad \tau \propto \frac{1}{l_{mfp}}$$

where l_{mfp} is the **mean free path** of a photon between collisions, I_0 is the intensity before absorption or scattering.

- $\tau \ll 1$ - optically thin
- $\tau \gg 1$ - optically thick

[1] Recall that intensity I is the energy emitted from a source surface element dA at position $\vec{\mathbf{r}}$, into solid angle $d\Omega$ in time interval between t and $t + dt$, i.e. $dE = I(\vec{\mathbf{r}})dAd\Omega dt$; **Specific intensity,** I_ν is the intensity in the frequency range ν and $\nu + d\nu$, i.e. $dE = I_\nu(\vec{\mathbf{r}})dAd\Omega dtd\nu$

3.3 Optically Thick and Thin Sources

Depending on optical depth within the emitting source, we distinguish:

Optically thick case:

Photons interact with, and are in thermal equilibrium with, hot gas e.g. **black-body radiation**

Optically thin case:

Gas does not appreciably absorb its own radiation. Observed spectrum of X-rays is same as spectrum during their production.

3.4 Bremsstrahlung

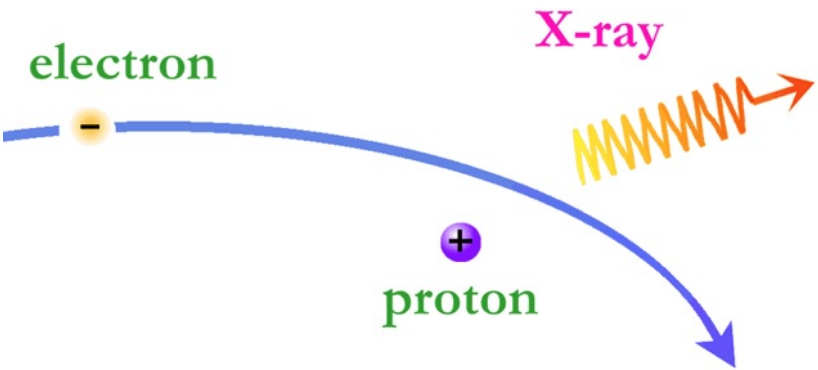

Figure 3.2: *Bremsstrahlung (free-free) emission in Hydrogen plasma. X-rays produced by* ***free-free transitions of electrons*** *also known as (thermal)* ***bremsstrahlung*** *(a.k.a 'braking radiation')*

Bremsstrahlung radiation could be due to either non-thermal electrons or thermal electrons, hence we distinguish **thermal** and **non-thermal bremsstrahlung**.

3.5 Non-Thermal bremsstrahlung

Emission of radiation by electrons with a Non-Maxwellian distribution of energies is called **Non-thermal bremsstrahlung**.

Usually a power-law energy distribution is a good model for non-thermal particles:

$$f(E) = CE^{-\delta}$$

where $f(E)dE$ is fraction (or number) of particles with energy between E and $E + dE$ and C and δ are constants.

So that the number density is

$$\text{Total number (or number density)} = \int_0^\infty f(E)dE$$

3.6 Inverse Compton Scattering

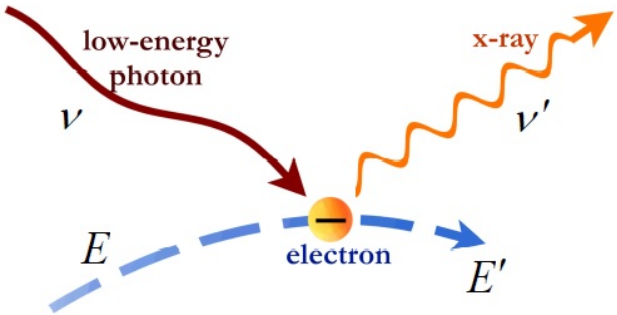

Figure 3.3: *Inverse Compton scattering*

Inverse Compton Scattering $\Longleftrightarrow$ A low energy photon collides with a relativistic electron and gains energy at the expense of the electron (e.g. radio photons might be boosted to X-ray energies)

For Inverse Compton scattering: $E' < E$ and $\nu' > \nu$

For Compton scattering: $E' > E$ and $\nu' < \nu$

For example, in the standard model of AGN, hot material forms above the accretion disc and can inverse-Compton scatter photons up to X-ray energies.

3.7 Synchrotron Radiation

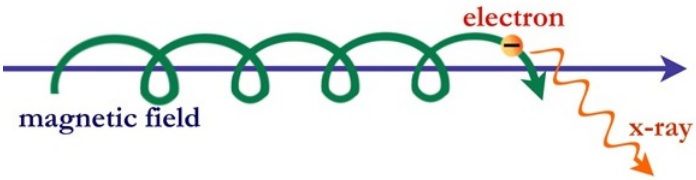

Figure 3.4: *Synchrotron Radiation*

Synchrotron Radiation $\Longleftrightarrow$ Emission of radiation by relativistic electrons spiralling in a magnetic field.

Radiation is normally **forward beamed** and **strongly polarised (generally only synchrotron has this property)**

For example, synchrotron radiation is responsible for X-ray emission from supernova remnants (e.g. Crab Nebula) and possibly X-ray continuum emission of quasars.

3.8 X-ray spectra shape

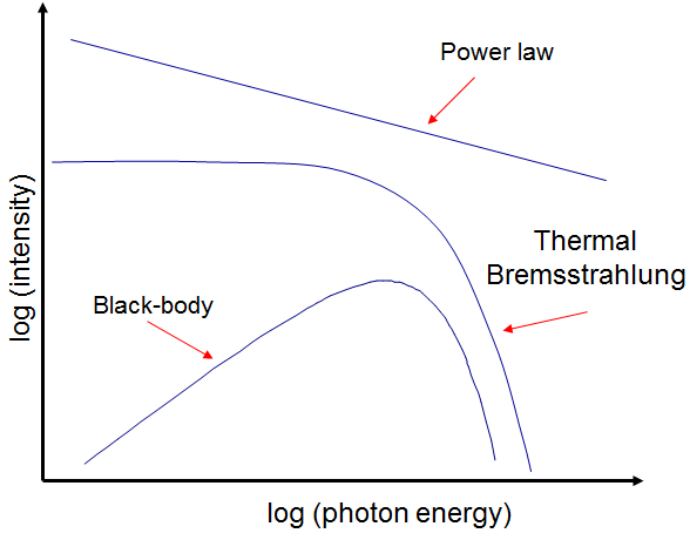

Figure 3.5: *Typical X-ray spectra.*

Power law X-ray spectrum may be generated by:

- Synchrotron radiation
- Inverse Compton
- Collisional bremsstrahlung

Spectrum which falls exponentially at high energies $\Longrightarrow$ **thermal**.

Many galactic sources appear to be thermal (Fig 3.7, 3.8), but other sources e.g. Crab Nebula (Fig 3.6) gives a power law spectrum.

3.9 Examples of X-ray spectra

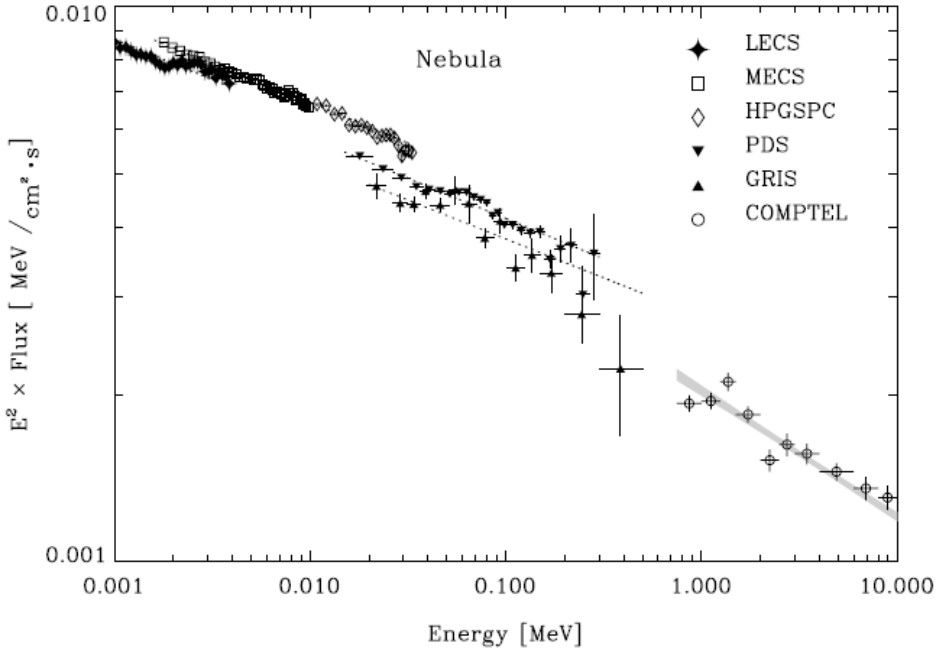

Figure 3.6: *The Crab nebula spectrum in the 1 keV - 10 MeV energy interval adopted from Kuiper, L. et al, 2001*

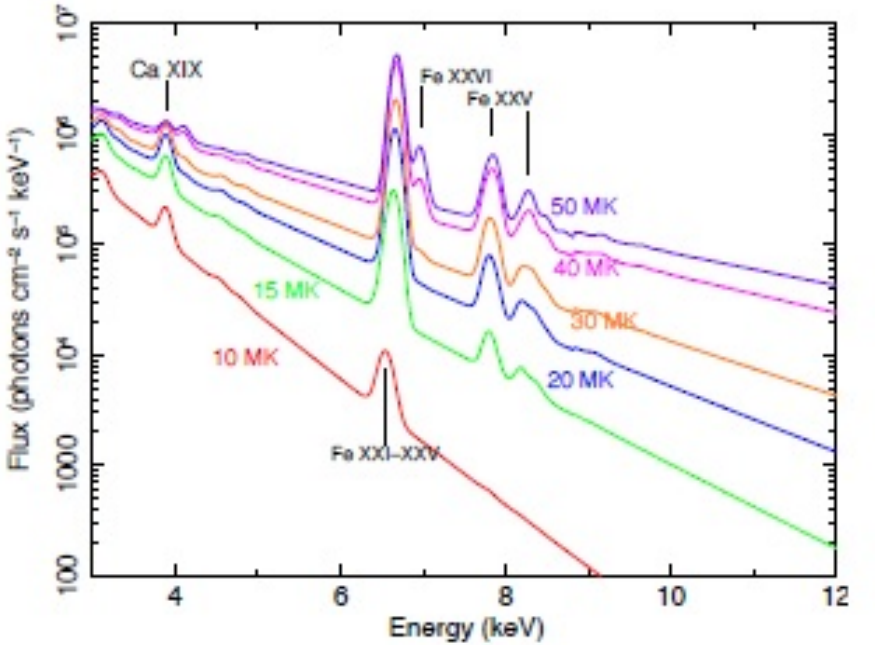

Figure 3.7: *Simulated X-ray spectra of solar flare plasma thermal emission for a range of plasma temperatures from 10 to 50 MK, from Skinner et al, 2013*

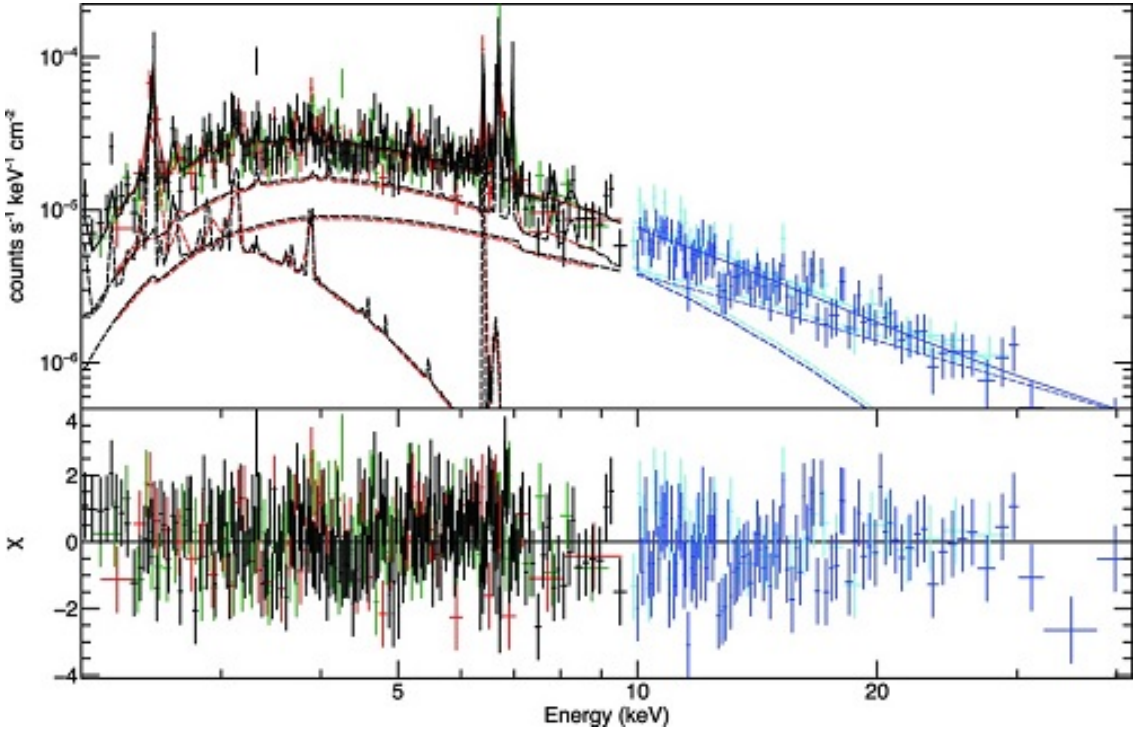

Figure 3.8: *Extended hard-X-ray emission from XMM-Newton and NuStar in the inner few parsecs of the Galaxy, from Perez et al, 2015*

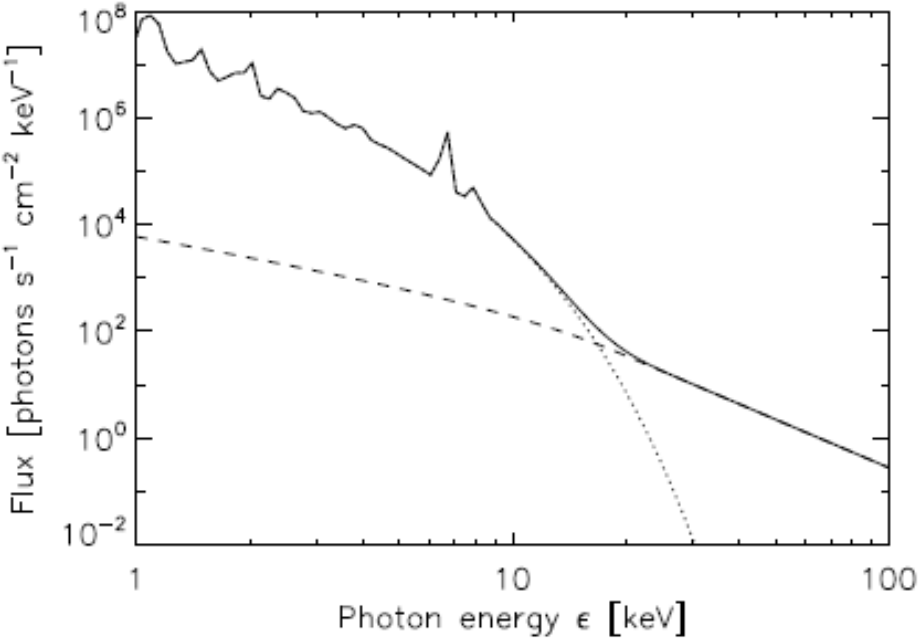

Figure 3.9: *Typical full-Sun flare X-ray spectrum. Dashed: non-thermal spectrum, Dotted: Thermal spectrum, from a plasma with temperature $T = 20$ MK, adopted from Holman et al, 2011*

3.10 Black-body emission

For Main Sequence stars, the peak of the black body curve lies in, or close to, the visible part of the E-M spectrum. For **X-ray sources**, peak lies at X-ray wavelengths. From **Wien's law:**

$$\lambda_{max} T = 2.9 \times 10^{-3} \qquad (3.1)$$

where λ_{max} [m], T [K]. For $T \simeq 10^7$ K, we find $\lambda_{max} \simeq 3$ Å, e.g. **classical X-rays**.

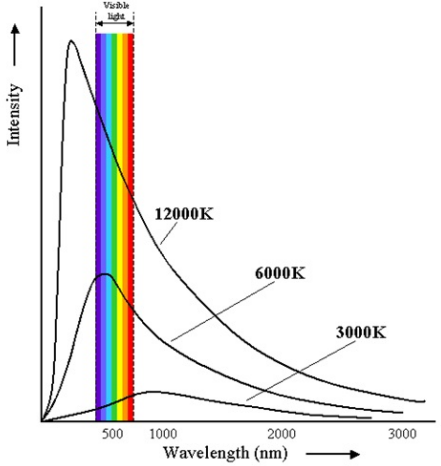

Figure 3.10: *Black-body spectra*

Planck Spectrum characterised by:

- Temperature of the source
- Isotropic emission
- Unpolarised radiation

3.11 Plank spectrum

Expressing **Planck spectrum** as a function of frequency:

$$I_\nu = \frac{2h\nu^3}{c^2\left[\exp\left(\frac{h\nu}{k_B T}\right) - 1\right]} \tag{3.2}$$

where I_ν is the specific intensity.

Limiting cases: For $h\nu \ll k_B T$, $\exp\left(\frac{h\nu}{k_B T}\right) - 1 \simeq \frac{h\nu}{k_B T}$ and

$$I_\nu \propto \nu^2 \quad \Longleftarrow \textbf{ Rayleigh-Jeans approximation} \tag{3.3}$$

For $h\nu \gg k_B T$, $\exp\left(\frac{h\nu}{k_B T}\right) - 1 \simeq \exp\left(\frac{h\nu}{k_B T}\right)$ and

$$I_\nu \propto \nu^3 \exp\left(-\frac{h\nu}{k_B T}\right) \quad \Longleftarrow \textbf{ Wien approximation} \tag{3.4}$$

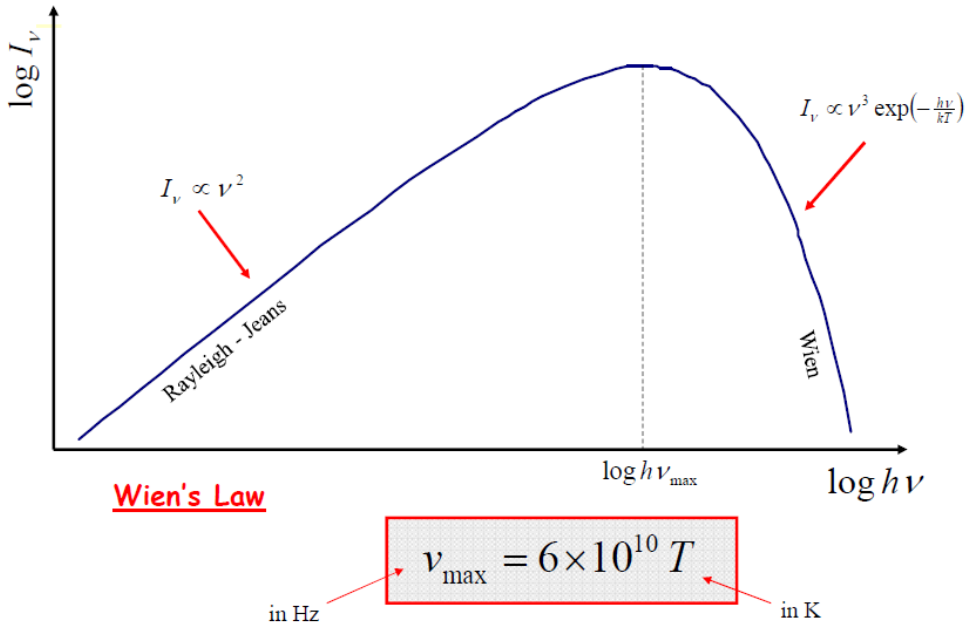

Figure 3.11: *Planck spectrum (Eq 3.2) and limiting cases (3.3, 3.4).*

3.12 Stefan-Boltzmann Law

Integrating the spectrum (3.2) over all frequencies, **bolometric luminosity** radiated per unit area from a black body becomes:

$$L_{bol} = \sigma T^4, \tag{3.5}$$

where $\sigma = 5.67 \times 10^{-8}$ Jm^{-2}s^{-1}K^{-4} is Stefan-Boltzmann constant.

Black body radiation energy density:

$$U_{rad} = aT^4 \tag{3.6}$$

where $a = \frac{4\sigma}{c} = 7.56 \times 10^{-16}$ Jm^{-3}K^{-4} is Stefan constant.

3.13 Black body emission from astrophysical objects

Consider a spherical mass, M, of radius, R, made of ionised hydrogen - dense enough to be optically thick, and hence emitting black body radiation, with $T \simeq 10^7$ K.

Suppose that T is uniform throughout the mass.

Thermal energy of the source is

$$E = 3Nk_BT$$

where N is the number of electrons (or protons).

Surface luminosity (e.g. power emitted) is

$$L = 4\pi R^2 \sigma T^4$$

Cooling time (using that $N = M/m_p$, where m_p is the proton mass)

$$\tau \simeq \frac{E}{L} = \frac{3kMT}{4\pi R^2 \sigma m_p T^4}$$

It can be shown that the cooling time

$$\tau = \frac{(140\text{sec}) \times \left(\frac{M}{M_\odot}\right)}{\left(\frac{R}{R_\odot}\right)^2 \times \left(\frac{T}{10^7\text{K}}\right)^3}$$

and the Luminosity

$$L = 3.5 \times 10^{39}\text{W} \times \left(\frac{R}{R_\odot}\right)^2 \times \left(\frac{T}{10^7\text{K}}\right)^4$$

and hence, for $T = 10^7$ K and $M = M_\odot$:

$$R = R_\odot \Longrightarrow \tau = 140\text{sec}\,; \quad L = 10^{13} L_\odot$$
$$R = 3 \times 10^{-3} R_\odot \Longrightarrow \tau = 6\text{months}\,; \quad L = 10^{8} L_\odot$$
$$R = 10^{-5} R_\odot \Longrightarrow \tau = 4 \times 10^{4}\text{years}\,; \quad L = 10^{3} L_\odot$$

3.14 Short and long-lived objects

Black body X-ray sources possible, with $M = M_\odot$, are:

- Small ($R \ll R_\odot$) long-lived compact objects
- Large ($R \sim R_\odot$) transient (short-lived) objects

3.15 Black body emission from astrophysical objects

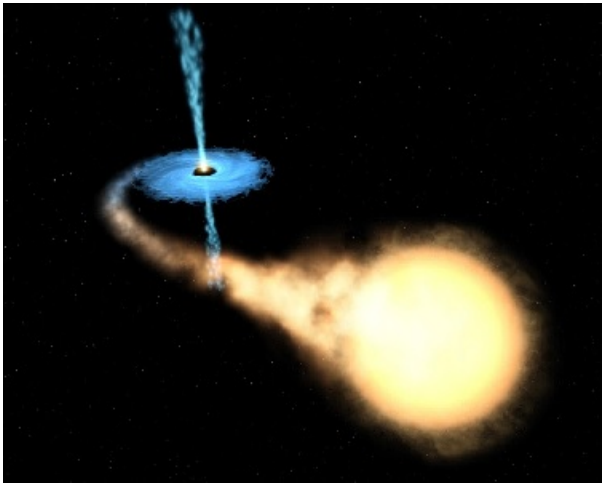

Figure 3.12: *NASA artist's impression of accretion disk*

In both cases (short and long-lived), we require high (or very high) luminosities, i.e. a source where energy is constantly supplied to maintain the luminosity $\Longrightarrow$ e.g. **Dense accretion disk in an X-ray binary**, see examples of X-ray spectra in Figures 3.13,3.14.

Also possible are very small, short lived sources with - e.g. X-ray bursts from the thermonuclear flash as newly accreted gas rich in hydrogen and helium reaches the neutron star surface.

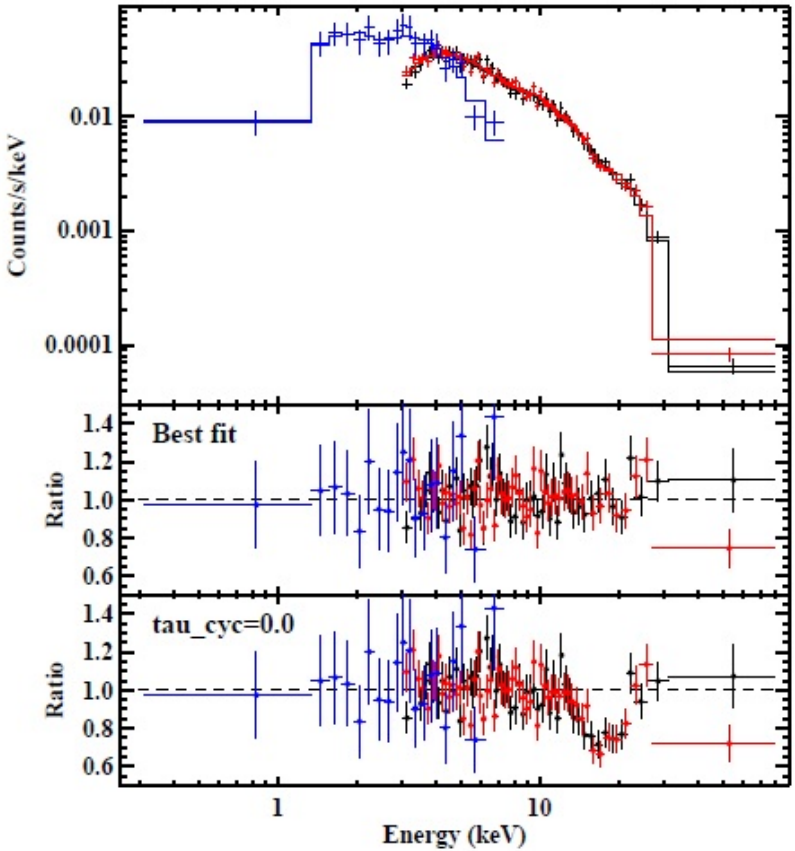

Figure 3.13: *Swift/XRT and NuSTAR spectrum (fitted with black-body) of the Supergiant Fast X-ray Transient IGR J17544-2619 from Tomsick et al, 2015*

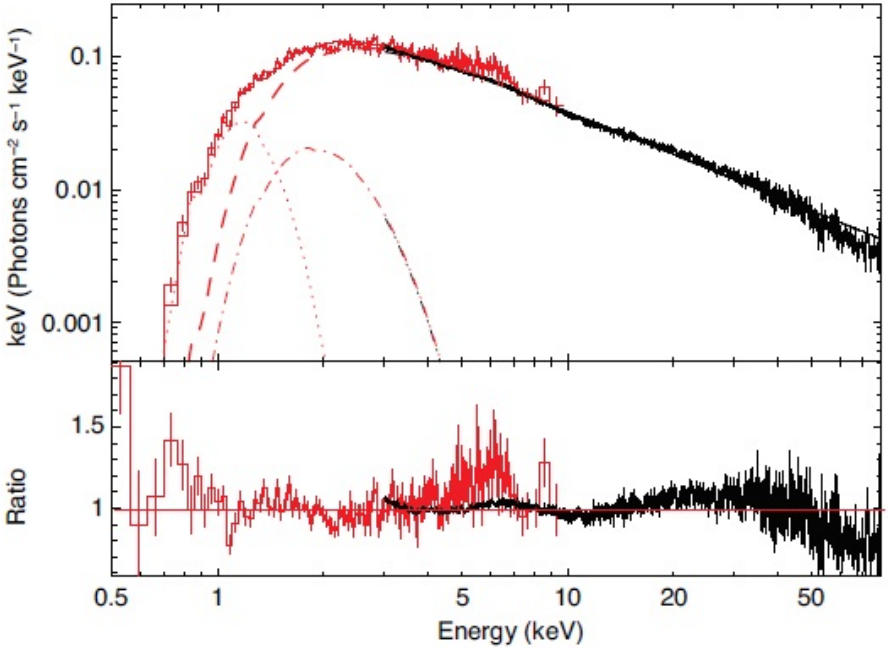

Figure 3.14: *Unfolded NuSTAR (black) and Swift (red) spectra from Degenaar et al, 2015. The solid lines indicate fits to an absorbed, phenomenological continuum consisting of a* $\Gamma = -2$ *power law (dashed lines), a cool* $k_B T_{bb} = 0.1$ *keV blackbody (dotted curve), and a hotter* $k_B T_{bb} = 0.4$ *keV blackbody (dash-dotted curves). The bottom panel shows the data-to-model ratio.*

4 Reaction cross-section

LECTURE OUTLINE

- Incident flux, reaction rate, reaction cross-section
- Emissivity, flux, luminosity
- Energy dependent characteristics (e.g. emissivity differential in energy)

4.1 Incident beam and target

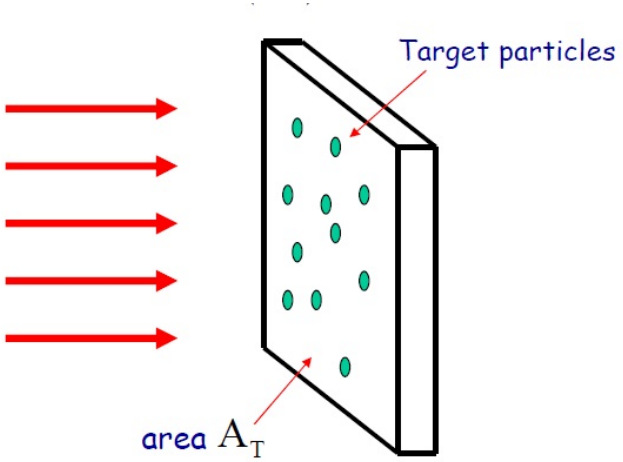

Figure 4.1: *Incident beam and target*

Consider a beam of particles (e.g. electrons) with number density, n [particles m^{-3}], and velocity v [m s^{-1}] incident on a thin 'target' containing N_T particles (e.g. protons) and with area A_T [m^{-2}] perpendicular to the incident beam (Fig. 4.1).

The total number of target particles

$$N_T = \int_V n_T(\vec{\mathbf{r}}) dV,$$

where $n_T(\vec{\mathbf{r}})$ is the target particle density (In general, it may depend on position within the target).

4.2 Incident flux and reaction rate

Incident flux is the number of beam particles crossing per unit area of the target per unit time

$$F = nv, \qquad [\text{particles m}^{-2}\ \text{s}^{-1}]$$

Reaction rate is number of interactions per unit time

$$R \propto FN_T, \qquad [\ \text{s}^{-1}]$$

4.3 Definition of reaction cross-section

We define the constant of proportionality to be the **reaction cross-section**, Q, which has units of area.

$$R = QFN_T$$

The reaction cross section can be thought of as defining an effective area for collisions/interactions between the beam and target particles.

Number of beam particles passing through target per unit time

$$= FA_T$$

Number of interactions per unit time is FN_TQ; Then

$$\textbf{Collision probability} = \frac{FN_TQ}{FA_T} = \frac{N_TQ}{A_T},$$

i.e. we can think of Q a disc of area associated with each target particle.

4.4 Definitions of emissivity

We are interested in interactions where a photon is emitted. We define the emission rate, or **emissivity**, J as the number of photons emitted per unit time from the interaction volume.

$$J = \int_V j(\vec{\mathbf{r}}) dV$$

where $j(\vec{\mathbf{r}})$ is the **emissivity per unit volume** (in general can depend on position within the target).

Then it follows that

$$j = n_T F Q \qquad [\mathrm{m}^{-3}\mathrm{s}^{-1}] \tag{4.1}$$

4.5 Energy dependent emissivity

Assuming that the incident flux of beam particles is independent of $\vec{\mathbf{r}}$ then

$$J = N_T F Q \tag{4.2}$$

Differential emissivity of photons with energy in the range between ϵ and $\epsilon + d\epsilon$ can be written as

$$dj = \frac{dj}{d\epsilon} d\epsilon$$

$$\frac{dj(\epsilon)}{d\epsilon} = n_T F \frac{dQ}{d\epsilon} \quad [\,\mathrm{m^{-3} s^{-1} keV^{-1}}] \tag{4.3}$$

where $\frac{dj(\epsilon)}{d\epsilon}$ is the differential emissivity of photons with energy, per unit energy range per unit volume, $\frac{dQ}{d\epsilon}$ is the **differential cross section**.

We can define **differential** quantities

$$j = \int_\epsilon \frac{dj}{d\epsilon} d\epsilon, \quad [\text{ photons m}^{-3}\text{s}^{-1}]$$

and

$$Q = \int_\epsilon \frac{dQ}{d\epsilon} d\epsilon, \quad [\text{ m}^2]$$

Similarly

$$\frac{dJ}{d\epsilon} = \int_V \frac{dj}{d\epsilon} dV, \quad [\text{ photons s}^{-1}\text{keV}^{-1}]$$

so that

$$J = \int_V \underbrace{\int_\epsilon \frac{dj}{d\epsilon} d\epsilon}_{=j} \, dV = \int_\epsilon \underbrace{\int_V \frac{dj}{d\epsilon} dV}_{=\frac{dJ}{d\epsilon}} \, d\epsilon$$

4.6 Source luminosity

The **differential source luminosity**, per unit photon energy range, is

$$\frac{dL}{d\epsilon} = \epsilon \frac{dJ}{d\epsilon}, \quad [\text{W keV}^{-1}] \tag{4.4}$$

Total source luminosity is then

$$L = \int_{\epsilon} \frac{dL}{d\epsilon} d\epsilon = \int_{\epsilon} \epsilon \frac{dJ}{d\epsilon} d\epsilon, \quad [\text{W}]$$

Combining with earlier results

$$L = \int_{\epsilon} \epsilon d\epsilon \int_{V} n_T F \frac{dQ}{d\epsilon} dV, \quad [\text{W}] \tag{4.5}$$

Note that more generally, the flux and cross section are a function of the energy of the incoming beam particles.

4.7 Angular dependence

Cross-section also quantifies the intrinsic rate at which the scattered particles (or emitted photons) can be detected at a given angle.

Spherical coordinate system is often used so that the target placed at the origin and the z-axis of aligned with the incident beam. Then

$$Q = \int_{\Omega} \frac{dQ}{d\Omega} d\Omega$$

where $d\Omega = \sin(\theta) d\theta d\varphi$, θ is the scattering angle, measured between the incident beam and the scattered beam, φ is the azimuthal angle. Often both energy and angular dependency are important, we have **energy and angle differential cross-section**,

$$\frac{d^2Q}{d\epsilon d\Omega}$$

so that the total cross-section Q is

$$Q = \int_{\Omega} \int_{\epsilon} \frac{d^2 Q}{d\epsilon d\Omega} d\epsilon d\Omega$$

4.8 Flux at the Earth

Note the distinction between the particle flux incident on the target and the flux received at the Earth

Consider a source at distance D. Then **photon number flux** at the Earth

$$\Psi = \frac{J}{4\pi D^2}, \quad [\,\mathrm{m^{-2}s^{-1}}]$$

and **energy flux** is

$$\Upsilon = \frac{L}{4\pi D^2}, \quad [\,\mathrm{Wm^{-2}}]$$

the corresponding **spectral distributions** are defined similarly to before (see Equations 4.3,4.4)

$$\frac{d\Psi}{d\epsilon} = \frac{1}{4\pi D^2}\frac{dJ}{d\epsilon}, \quad [\,\mathrm{m^{-2}s^{-1}keV^{-1}}]$$

$$\frac{d\Upsilon}{d\epsilon} = \frac{1}{4\pi D^2}\frac{dL}{d\epsilon} = \frac{\epsilon}{4\pi D^2}\frac{dJ}{d\epsilon}, \quad [\,\mathrm{J\,m^{-2}s^{-1}keV^{-1}}]$$

4.9 Note different differential characteristics

Some characteristics are presented in the table below[2]

Quantity/chacteristic	Integrated (e.g. energy integrated)	differential
luminosity	L	$\frac{dL}{d\varepsilon}$
emissivity	$J = L/\varepsilon$	$\frac{dJ}{d\varepsilon}$
emissivity per unit volume	j	$\frac{dj}{d\varepsilon}$
cross-section	Q	$\frac{dQ}{d\varepsilon}$
cross-section	Q	$\frac{dQ}{d\varepsilon d\Omega}$
...	...	...

[2] At home, complete the table with various values used in the course.

5 Thomson scattering

LECTURE OUTLINE

- Classical treatment of wave scattering
- Thomson scattering, cross-section
- Limitations of classical description

5.1 EM wave scattering

Thomson scattering is the classical, non-relativistic scattering of radiation by a free electron - at rest initially - accelerated by interaction with the radiation to velocity v.

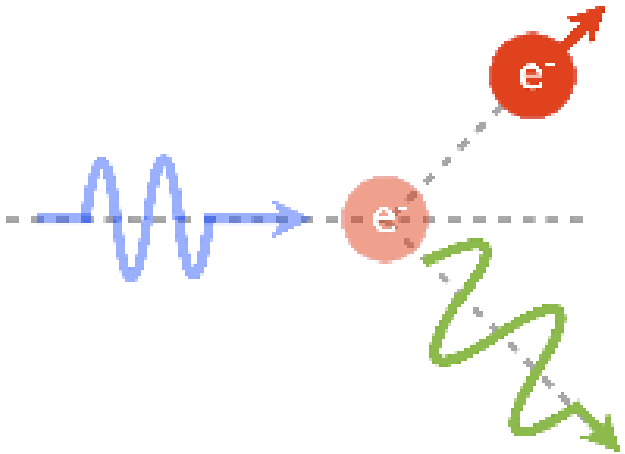

Figure 5.1: *Cartoon showing scattering of EM wave on a free electron from Jeffrey (2014)*

Classically, the $\vec{\mathbf{E}}$-field exerts a force on the electron (we can neglect the $\vec{\mathbf{B}}$-field if $v \ll c$, where c is the speed of light)

We assume $\vec{\mathbf{E}} = \vec{\mathbf{E}}_0 \cos(\omega t)$ at the electron, which we treat as a single particle target (i.e. with $N_T = 1$)

5.2 Incoming EM flux

Incident energy flux (modulus of Poynting vector, $\vec{\mathbf{S}}$),

$$S = \left|\vec{\mathbf{S}}\right| = \left|\frac{1}{\mu_0}\vec{\mathbf{E}} \times \vec{\mathbf{B}}\right| = \frac{1}{2} c \epsilon_0 E_0^2, \quad [\mathrm{W\ m^{-2}}] \tag{5.1}$$

where ϵ_0 is the dielectric permittivity of free space, μ_0 is the vacuum permeability.

Then **incident photon flux**,

$$F = \frac{S}{\hbar\omega}, \quad [\mathrm{photons\ s^{-1} m^{-2}}]$$

where

$$\hbar \equiv \frac{h}{2\pi}.$$

5.3 Radiated EM emission

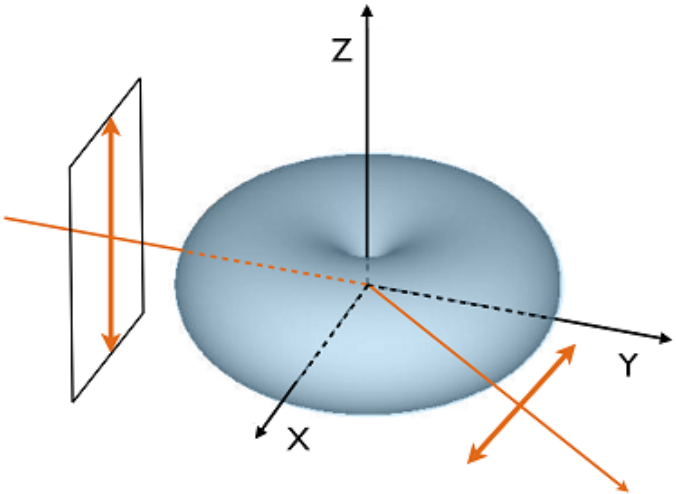

Figure 5.2: *Cartoon showing a polarized incident plane wave interacting with an electron, causing it to oscillate and re-radiate. The original figure was taken from here and Jeffrey (2014).*

Power radiated by scattered electron (e.g. by charge moving with acceleration $\dot{v}$)

$$P = \frac{e^2 \dot{v}^2}{6\pi\epsilon_0 c^3}, \quad [\,\mathrm{W}\,] \qquad (5.2)$$

where e is the electron charge.

We know that from 2-nd Newton law

$$m\dot{\vec{\mathbf{v}}} = e\vec{\mathbf{E}},$$

where m is the electron mass. Hence one finds

$$\dot{v}^2 = \frac{e^2 E_0^2 \cos^2 \omega t}{m^2}$$

and averaging over a wave period $T = 2\pi/\omega$

$$\langle \dot{v}^2 \rangle = \frac{e^2 E_0^2}{m^2} \underbrace{\langle \cos^2 \omega t \rangle}_{=1/2} = \frac{e^2 E_0^2}{2m^2}$$

therefore power radiated by oscillating electron is

$$P = \frac{e^4 E_0^2}{12\pi\epsilon_0 m^2 c^3}, \quad [\text{ W}] \tag{5.3}$$

Classically, scattered radiation also has angular frequency ω (i.e. **elastic scattering** of electromagnetic radiation and energy is not transferred to the scattering electron)

Then photon emissivity is

$$J = \frac{P}{\hbar\omega}, \quad [\text{ photons s}^{-1}]$$

But we also have

$$J = N_T F Q = \underbrace{1}_{=N_T} \frac{S}{\underbrace{\hbar\omega}_{=F}} Q$$

since on the other hand we have

$$J = \frac{P}{\hbar\omega}$$

hence

$$Q = \frac{P}{S}$$

Substituting expressions for S (Eq 5.1) and P (Eq. 5.3), one finds

$$Q = \frac{P}{S} = \underbrace{\frac{e^4 E_0^2}{12\pi\epsilon_0 m^2 c^3}}_{=P} \underbrace{\frac{2}{c\epsilon_0 E_0^2}}_{=1/S}$$

simplifying, we find the expression for the cross-section.

Thomson cross-section:

$$Q_T = \frac{8\pi}{3}\left(\frac{e^2}{4\pi\epsilon_0 mc^2}\right)^2 = \frac{8\pi}{3}r_e^2 \qquad (5.4)$$

where r_e is the **classical electron radius**. Numerically

$$Q_T = 6.65 \times 10^{-29} \ \ \mathrm{m}^2$$

in SI units.

5.4 Classical electron radius

The classical electron radius, r_e, is the length scale at which the electrostatic (Coulomb) energy of an electron is equal to its rest-mass energy.

Let us consider two electrons, A and B (which classically we think of as point particles) separated by distance r_e.

Electrostatic energy of A, due to Coulomb repulsion of B (and vice versa) is given by

$$\frac{e^2}{4\pi\epsilon_0 r_e}$$

Equating it to mc^2, we have

$$\frac{e^2}{4\pi\epsilon_0 r_e} = mc^2$$

hence, one finds

$$r_e = \frac{e^2}{4\pi\epsilon_0 mc^2} = 2.82 \times 10^{-15}\text{m}$$

Classically, therefore, we can think of as the cross-sectional area of the 'disc' over which the pointlike electron influences other particles in its vicinity.

r_e is (**approximately**) the radius of this disc.

BUT:

How does this classical picture of the disc around the electron fit in with its quantum description?

5.5 Limitations of classical description

Take electron momentum, $p \simeq mc$

Equate this with Δp from the **Heisenberg uncertainty principle**, (e.g. $\Delta p \Delta x \geq \hbar/2$)

$$mc \simeq \Delta p \geq \frac{\hbar}{\Delta x}$$

This lets us define a 'Quantum' length scale:

$$\lambda_Q \simeq \Delta x \geq \frac{\hbar}{mc} = \frac{4\pi\epsilon_0 c\hbar}{e^2} r_e \tag{5.5}$$

The quantity

$$\alpha = \frac{e^2}{4\pi\epsilon_0 c\hbar} \simeq \frac{1}{137}$$

is a dimensionless number known as the **fine structure constant**.

So from Equation (5.5), we find for high-energy electrons quantum effects become important on a scale

$$\lambda_Q \lesssim \frac{1}{\alpha} r_e \simeq 137 r_e$$

The Thomson cross-section is, however, an adequate description of low energy scattering:

$$\hbar\omega \ll mc^2$$

This is consistent with the assumption of elastic scattering or small energy exchange, i.e. the electron kinetic energy and photon frequency are the same before and after the scattering.

6 Bremsstrahlung

LECTURE OUTLINE

- Bremsstrahlung emission mechanism
- Differential bremsstrahlung cross-section
- Bethe-Heitler formula
- Optically thin spectrum and bremsstrahlung luminosity spectrum
- Non-thermal bremsstrahlung

6.1 Bremsstrahlung emission mechanism

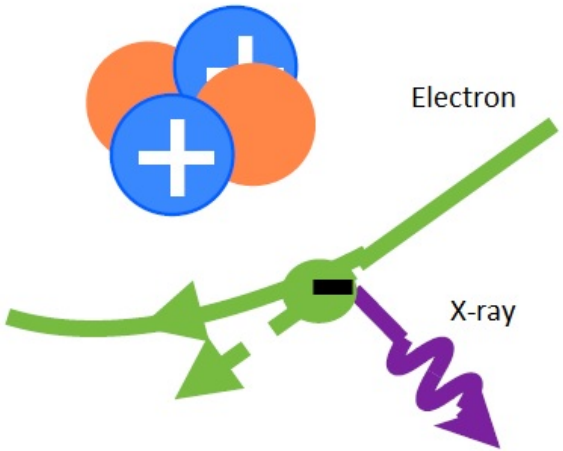

Figure 6.1: *Cartoon showing bremsstrahlung emission on an ion from Jeffrey (2014)*

Bremsstrahlung radiation is produced from the interaction of electrons with a proton (or ion, see Fig 6.1).

For X-ray production, we want an electron which is **fast** but still **non-relativistic**.

Consider an electron with kinetic energy, $E = 10$ keV.

Compare this with the electron's rest mass energy:

$$\frac{mv^2/2}{mc^2} = 0.02 \Longrightarrow \frac{v^2}{c^2} = 0.04 \Longrightarrow v = 0.2c$$

6.2 Differential electron flux

Consider a plasma of ionised hydrogen, with a proton density n_p m^{-3}. Note that the electron density $n_e = n_p$.

For electrons with a single speed (monoenergetic beam) v, and kinetic energy $E = mv^2/2$

$$\textbf{Electron flux} = n_e v \quad [\text{m}^{-2}\text{s}^{-1}]$$

Suppose now we have a distribution of electron speeds. Total electron flux

$$F_{tot} = \int_E \frac{dF}{dE} dE, \qquad [\text{electron m}^{-2}\text{s}^{-1}]$$

where **differential flux or flux spectrum**

$$\frac{dF}{dE} \equiv F(E), \quad [\text{electron m}^{-2}\text{s}^{-1}\text{keV}^{-1}] \quad \textbf{flux spectrum}$$

$F(E)dE$ is the flux of electrons [$m^{-2}s^{-1}$] with kinetic energy in the range between E and $E + dE$

$$F(E) = v(E)\frac{dn_e}{dE}$$

where $v(E) = \sqrt{2E/m}$ and

$$\frac{dn_e}{dE} = \text{number of electrons [} m^{-3}keV^{-1}]$$

6.3 Differential emissivity

Differential emissivity for photons of energy ϵ produced by electrons of a single energy (speed) $E = mv^2/2$ is given by

$$\frac{dj}{d\epsilon} = n_p F \frac{dQ_B}{d\epsilon}(\epsilon, E) \quad \text{[photons m}^{-3}\text{s}^{-1}\text{keV}^{-1}\text{]} \tag{6.1}$$

where $F = n_e v$ and

$$\frac{dQ_B}{d\epsilon}(\epsilon, E) \Longleftrightarrow \textbf{differential bremsstrahlung cross-section}$$

i.e. cross-section for photon emission in energy range $(\epsilon, \epsilon + d\epsilon)$ from an electron with energy E. The units are [m^2 keV^{-1}].

Suppose now we have a distribution of electron speeds, then we need to sum the contributions from all electron energies, i.e. to integrate equation (6.1).

The emissivity differential in energy becomes:

$$\frac{dj}{d\epsilon} = n_p \int_{\epsilon}^{\infty} F(E) \frac{dQ_B}{d\epsilon}(\epsilon, E) dE \quad [\text{ photons m}^{-3}\text{s}^{-1}\text{keV}^{-1}] \qquad (6.2)$$

Note that the integral lower limit arises from **energy conservation** - i.e. each emitted photon cannot have more energy than the kinetic energy of the electron whose deceleration produced it.

We compute the emissivity for photons of energy ϵ by integrating over all electrons with energy $E > \epsilon$.

6.4 Bremsstrahlung cross-section

Bremsstrahlung cross-section can be written

$$\frac{dQ_B}{d\epsilon}(\epsilon, E) = \frac{Q_0 mc^2}{\epsilon E} \ln\left(\frac{1+\sqrt{1-\epsilon/E}}{1-\sqrt{1-\epsilon/E}}\right) \tag{6.3}$$

This is known as the **Bethe-Heitler** formula, where

$$Q_0 = \frac{8}{3}\alpha r_e^2 = 1.54 \times 10^{-31}\,[\mathrm{m}^2]$$

recalling that $\alpha = 1/137$, we find that

$$Q_0 = \frac{Q_T}{137\pi}$$

The Bethe-Heitler formula is valid in the regime where the initial v_i and final

v_f velocities of the electron satisfy:

$$\alpha c \ll v_i, \quad v_f \ll c$$

(For lower v_i velocities we require quantum mechanical corrections; for higher velocities we require relativistic corrections)

Note that the term

$$\ln\left(\frac{1+\sqrt{1-\epsilon/E}}{1-\sqrt{1-\epsilon/E}}\right)$$

is rather complicated (see Fig 6.2).

This factor should be included in precise calculations (e.g. RHESSI), but it varies fairly slowly with and we will replace it by a constant.

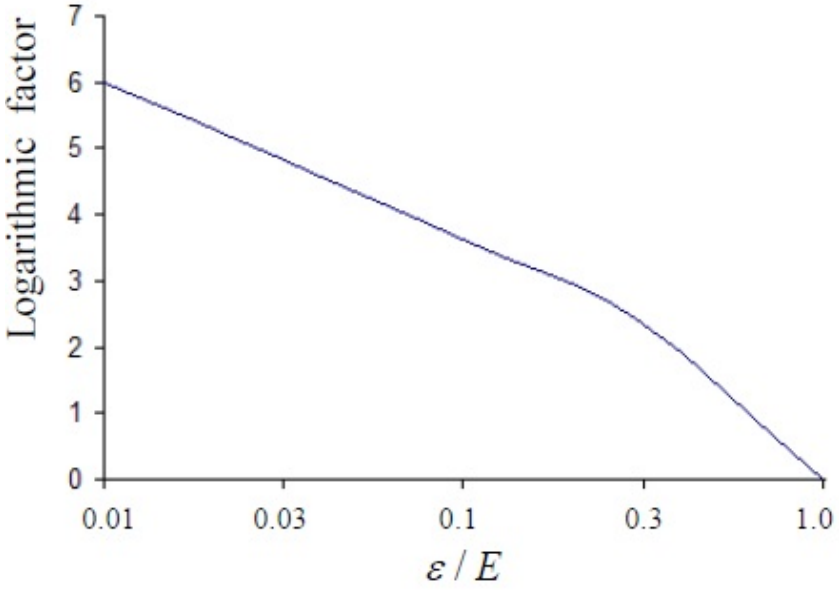

Figure 6.2: *Log-term* $\ln\left(\frac{1+\sqrt{1-\epsilon/E}}{1-\sqrt{1-\epsilon/E}}\right)$ *from Eq. 6.3.*

For simplicity we can take,

$$\ln\left(\frac{1+\sqrt{1-\epsilon/E}}{1-\sqrt{1-\epsilon/E}}\right) = 1$$

so that bremsstrahlung cross-section can be written

$$\frac{dQ_B}{d\epsilon}(\epsilon, E) = \frac{Q_0 mc^2}{\epsilon E} \quad [\mathrm{m^2 keV^{-1}}] \tag{6.4}$$

This is known as the **Kramers** approximation.

6.5 Optically thin spectrum

Substituting Equation (6.4) into the expression for differential emissivity (Eq. 6.1), one finds a simplified expression:

$$\frac{dj}{d\epsilon} = n_p \frac{Q_0 mc^2}{\epsilon} \int_{\epsilon}^{\infty} \frac{F(E)}{E} dE \quad [\text{ photons m}^{-3}\text{s}^{-1}\text{keV}^{-1}]$$

For an **extended, optically thin** source of volume V, in which we have $n_p = n_p(\vec{\mathbf{r}})$, $F(E) = F(E, \vec{\mathbf{r}})$, i.e. proton number density and electron energy distribution are, in general, functions of position.

The bremsstrahlung **differential emissivity** is (using Kramers approximation)

$$\frac{dJ}{d\epsilon} = \frac{Q_0 mc^2}{\epsilon} \int_V n_p(\vec{\mathbf{r}}) \int_\epsilon^\infty \frac{F(E,\vec{\mathbf{r}})}{E} dE dV \quad [\text{ photons s}^{-1}\text{keV}^{-1}] \quad (6.5)$$

and

the **differential luminosity** becomes

$$\frac{dL}{d\epsilon} = \epsilon \frac{dJ}{d\epsilon} = Q_0 mc^2 \int_V n_p(\vec{\mathbf{r}}) \int_\epsilon^\infty \frac{F(E,\vec{\mathbf{r}})}{E} dE dV \quad [\text{ J s}^{-1}\text{keV}^{-1}] \quad (6.6)$$

We will apply these formulae later, and in the example sheets.

6.6 Bremsstrahlung luminosity spectrum

Suppose there exists some non-zero energy, E_{min}, such that the kinetic energy of all electrons satisfies $E > E_{min}$.

It then follows that $F(E, \vec{\mathbf{r}}) = 0$, for all $E < E_{min}$, and the energy integral in Equation 6.6

$$\int_{\epsilon}^{\infty} \frac{F(E, \vec{\mathbf{r}})}{E} dE = \int_{E_{min}}^{\infty} \frac{F(E, \vec{\mathbf{r}})}{E} dE$$

Hence, for all photon energies $\epsilon < E_{min}$, the differential emissivity

$$\frac{dJ}{d\epsilon} = \frac{Q_0 mc^2}{\epsilon} \int_V n_p(\vec{\mathbf{r}}) \int_{E_{min}}^{\infty} \frac{F(E, \vec{\mathbf{r}})}{E} dE dV \quad [\text{ photons s}^{-1}\text{keV}^{-1}]$$

and the luminosity

$$\frac{dL}{d\epsilon} = Q_0 mc^2 \int_V n_p(\vec{\mathbf{r}}) \int_{E_{min}}^{\infty} \frac{F(E,\vec{\mathbf{r}})}{E} dE dV \quad [\text{J s}^{-1}\text{keV}^{-1}]$$

Note that $\frac{dL}{d\epsilon}$ is independent of the photon energy ϵ.

Hence at low photon energies, $\epsilon < E_{min}$, the differential bremsstrahlung spectrum, $\frac{dL}{d\epsilon}$, is **flat**.

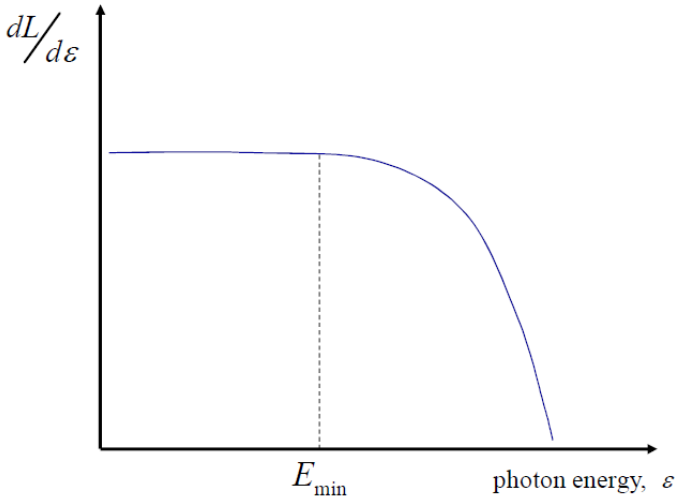

Figure 6.3: *For a* ***thermal distribution of electrons****, we have* $F(E) \longrightarrow 0$ *as* $E \longrightarrow 0$*, so we can make the approximation* $F(E,\vec{\mathbf{r}}) = 0$*, for all* $E < E_{min}$ *and and hence the luminosity spectrum of thermal bremsstrahlung becomes flat at low photon energies.*

6.7 Non-thermal bremsstrahlung

Consider a non-Maxwellian distribution of electron velocities - e.g. a power law differential electron flux spectrum:

$$F(E) = F_0 E^{-\delta}$$

where $F(E)dE$ is the fraction (or number) of particles with energy between E and $E + dE$, and F_0 and δ.

Note that the power law is usually defined from some low energy cut off, E_{min}, because a power law extending to $E \longrightarrow 0$ would formally give $F(E) \longrightarrow \infty$ for $\delta > 0$.

Consider electrons with kinetic energy $E > E_{min}$. Total flux for $\delta > 1$

$$F_{tot} = \int_{E_{min}}^{\infty} F(E)dE = \int_{E_{min}}^{\infty} F_0 E^{-\delta} dE = \frac{F_0}{1-\delta} E^{1-\delta}\Big|_{E_{min}}^{\infty} = \frac{F_0}{\delta - 1} E_{min}^{1-\delta}$$

i.e. we find the constant

$$F_0 = F_{tot}(\delta - 1)E_{min}^{\delta-1}$$

where F_{tot} is the flux above E_{min}.

Differential emissivity with power-law flux spectrum of electrons is, then:

$$\frac{dJ}{d\epsilon} = \frac{Q_0 mc^2}{\epsilon} \int_V n_p(\vec{\mathbf{r}}) \int_\epsilon^\infty \frac{F_0 E^{-\delta}}{E} dE dV$$

$$\frac{dJ}{d\epsilon} = \frac{Q_0 mc^2}{\epsilon} \int_V n_p(\vec{\mathbf{r}}) \int_\epsilon^\infty F_0 E^{-\delta-1} dE dV$$

which is valid for $E > E_{min}$.

For a **uniform plasma** with $n_p(\vec{\mathbf{r}}) = const = n_p$ and F_0, δ are constant,

$$\frac{dJ}{d\epsilon} = \frac{Q_0 mc^2}{\epsilon} n_p V F_0 \left(-\frac{E^{-\delta}}{\delta} \right) \Bigg|_{\epsilon}^{\infty}$$

The volume-integrated emissivity differential in energy becomes

$$\frac{dJ}{d\epsilon} = \frac{Q_0 mc^2}{\delta} n_p V F_0 \epsilon^{-(\delta+1)} \qquad (6.7)$$

hence

$$\frac{dJ}{d\epsilon} \propto \epsilon^{-(\delta+1)}; \quad \frac{dL}{d\epsilon} = \epsilon \frac{dJ}{d\epsilon} \propto \epsilon^{-\delta}$$

Thus, the non-thermal (collisional) bremsstrahlung photon spectrum is **also a power law**, with the same exponent as the power law differential electron flux spectrum. **Observationally**, by measuring the slope of the observed photon spectrum, we can deduce the slope of the electron flux spectrum.

7 Thermal and multi-thermal bremsstrahlung

LECTURE OUTLINE

- Thermal Bremsstrahlung
- Non-uniform, non-isothermal plasma
- Multi-thermal bremsstrahlung

7.1 Isothermal, uniform plasma

Consider an isothermal, homogeneous plasma of fully ionised hydrogen. We have $n_e = n_p$ independent of position

$$F(E) = F_M(E) = v(E)\frac{dn_e}{dE}$$

where $\frac{dn_e}{dE}$ is the Maxwellian distribution. Hence the flux spectrum

$$F_M(E) = \sqrt{\frac{2E}{m}}\frac{2n_p}{\sqrt{\pi}}\frac{E^{1/2}}{(k_B T)^{3/2}}\exp\left(-\frac{E}{k_B T}\right)$$

Note: before we defined $F(E) = F(E, \vec{\mathbf{r}})$, this is equivalent to writing $F(E) = F(E, T)$ provided we can define $T = T(\vec{\mathbf{r}})$.

The differential emissivity is, then

$$\frac{dJ}{d\epsilon} = \frac{Q_0 mc^2}{\epsilon} \int_V n_p(\vec{\mathbf{r}}) \int_\epsilon^\infty \frac{F(E,T)}{E} dE dV =$$

$$= \frac{2 n_p^2 V Q_0 mc^2}{\epsilon} \int_\epsilon^\infty \sqrt{\frac{2}{\pi m}} \frac{E}{E} \frac{1}{(k_B T)^{3/2}} \exp\left(-\frac{E}{k_B T}\right) dE \,.$$

Putting $z = E/k_B T$ and integrating over E,

the emissivity spectrum becomes

$$\frac{dJ}{d\epsilon} = 2\sqrt{\frac{2}{\pi m}}\frac{n_p^2 V Q_0 mc^2}{(k_B T)^{1/2}\epsilon}\exp\left(-\frac{\epsilon}{k_B T}\right) \tag{7.1}$$

and luminosity spectrum

$$\frac{dL}{d\epsilon} = 2\sqrt{\frac{2}{\pi m}}\frac{n_p^2 V Q_0 mc^2}{(k_B T)^{1/2}}\exp\left(-\frac{\epsilon}{k_B T}\right) \tag{7.2}$$

Thus, the energy spectrum for **thermal bremsstrahlung** from a homogeneous plasma decays **exponentially** at high photon energies.

7.2 Spectral shape

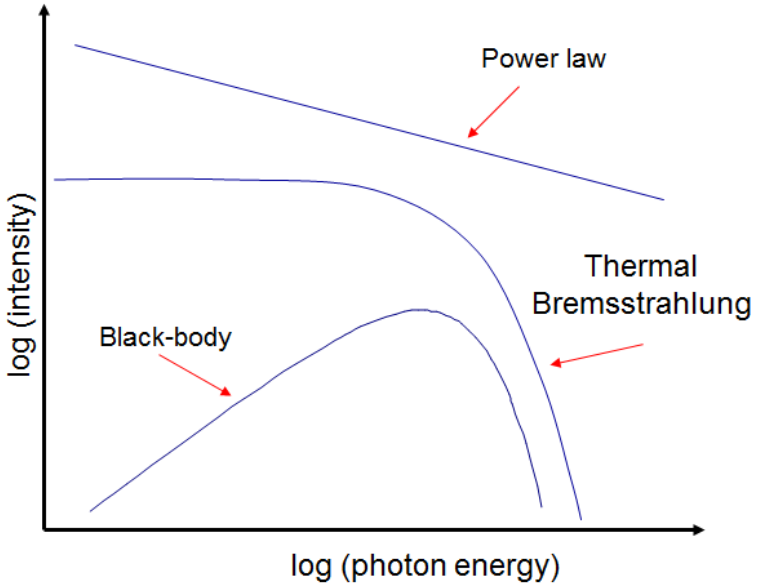

Recall Figure 3.5 from the previous lectures.

Spectrum which falls exponentially at high energies - **thermal**, see e.g. Figure 3.5.

Observationally, measuring the shape of $\frac{dL}{d\epsilon}$ allows us to determine a temperature, T, for the plasma. We can do this, e.g., for the X-ray emission from galaxy clusters and the Sun. (The isothermal assumption may break down, however).

7.3 Thermal bremsstrahlung from Coma cluster

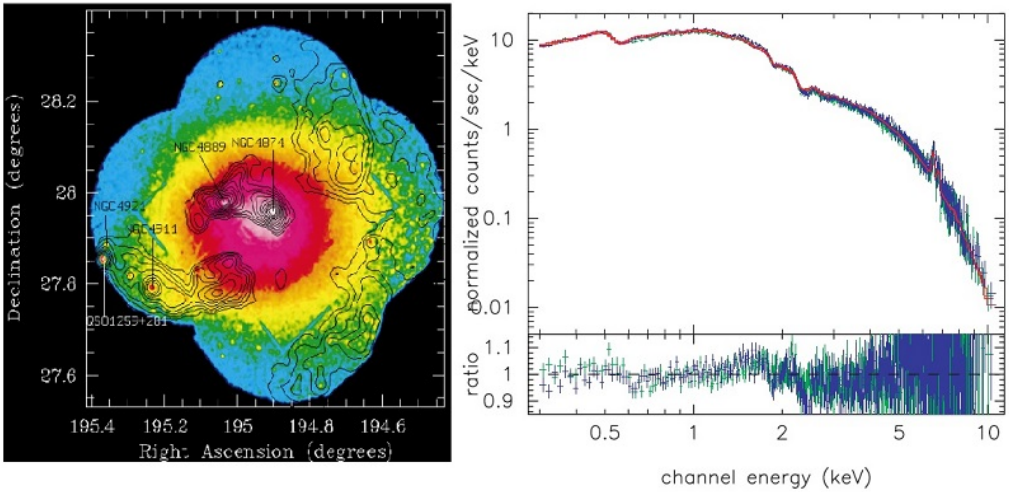

Figure 7.1: *XMM-Newton mosaic image of the central region of Coma (5 overlapping pointings) in the [0.3-2] keV energy band and isothermal with with* $k_B T = 8.25$ *keV from Arnaud et al, 2001*

7.4 Thermal (and non-thermal) bremsstrahlung from solar flares

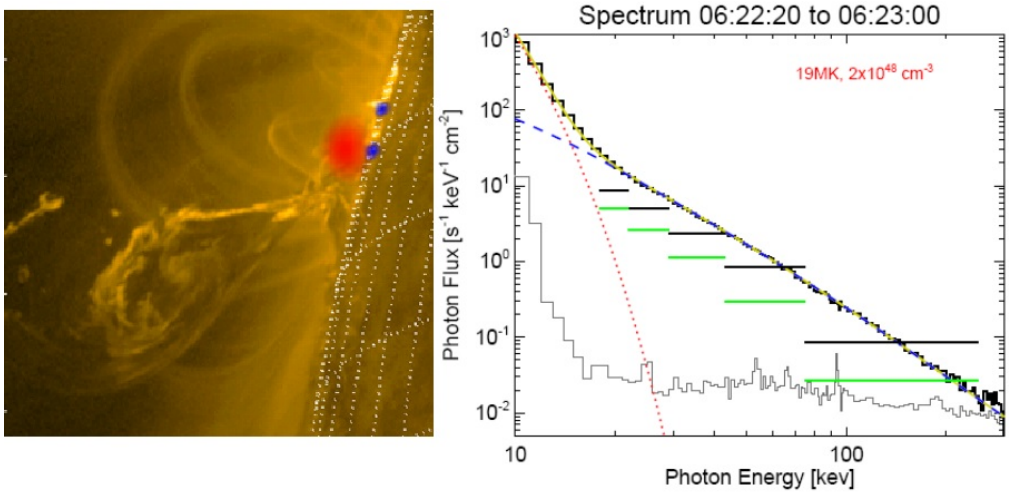

Figure 7.2: *Left: RHESSI image of a solar flare: red - thermal, blue - non-thermal, yellow background is* ~ 1 *MK plasma from SDO/AIA; Right: X-ray spectrum of a limb flare. From Kontar et al, 2010*

7.5 Multi-Thermal Bremsstrahlung

Recall Equation 7.2 for thermal bremsstrahlung:

$$\frac{dL}{d\epsilon} = 2\sqrt{\frac{2}{\pi m}}\frac{n_p^2 V Q_0 m c^2}{(k_B T)^{1/2}} \exp\left(-\frac{\epsilon}{k_B T}\right)$$

Measuring $dL/d\epsilon$ also permits us to determine $n_p^2 V$. This quantity is known as the **emission measure**.

Note that the mass of gas in the plasma is given by (ignoring the mass of electrons): $M_{gas} = n_p V m_p$.

So the emission measure does not directly tell us M_{gas}; to determine this we need to estimate V separately.

For example, for the X-ray emission from a galaxy cluster, we can assume the cluster is spherical and use its angular size and redshift to estimate its volume.

7.6 Inhomogeneous plasma

Suppose the plasma is **not isothermal**. Consider the differential emissivity per unit volume at position, $\vec{\mathbf{r}}$ (from Equation 7.1)

$$\frac{dj}{d\epsilon} = 2\sqrt{\frac{2}{\pi m}}\frac{n_p^2(\vec{\mathbf{r}})Q_0 mc^2}{(k_B T(\vec{\mathbf{r}}))^{1/2}\epsilon}\exp\left(-\frac{\epsilon}{k_B T(\vec{\mathbf{r}})}\right) \quad [\text{ photons m}^{-3}\text{s}^{-1}\text{keV}^{-1}]$$

Integrated emissivity for the whole volume is then

$$\frac{dJ}{d\epsilon} = \int_V \frac{dj}{d\epsilon} dV$$

i.e.

$$\frac{dJ}{d\epsilon} = 2\sqrt{\frac{2}{\pi m}}\frac{Q_0 mc^2}{k^{1/2}\epsilon}\int_V \frac{n_p^2(\vec{\mathbf{r}})}{T(\vec{\mathbf{r}})^{1/2}}\exp\left(-\frac{\epsilon}{k_B T(\vec{\mathbf{r}})}\right) dV$$

7.7 Source emission measure function

One useful approach to simplifying this expression is to replace the integral over volume with an integral over temperature. We do this by introducing **the source emission measure function** or sometimes called **differential emission measure**. This is a measure of how much of the plasma is at temperature T.

We define

$$\int_T \xi(T) dT = \int_V n_p^2(\vec{\mathbf{r}}) dV \tag{7.3}$$

where $\vec{\mathbf{r}} = \vec{\mathbf{r}}(T)$.

From which it can be shown that (e.g. using integration by parts)[3],

[3] Try at home as exercise

the differential emissivity from inhomogeneous, non-isothermal plasma becomes

$$\frac{dJ}{d\epsilon} = 2\sqrt{\frac{2}{\pi m}}\frac{Q_0 mc^2}{k^{1/2}\epsilon}\int_0^\infty \xi(T)\frac{1}{T^{1/2}}\exp\left(-\frac{\epsilon}{k_B T}\right)dT \qquad (7.4)$$

where $\xi(T)$ characterises the plasma.

7.8 Spherical volume

We can see more easily how this substitution works for the specific example of a spherically symmetric temperature distribution, i.e.

$$T = T(r)$$

We make the change of variables from (r, θ, φ) to (T, θ, φ) and we write

$$dV = r^2 \sin(\theta) d\theta d\varphi dr = dS dr$$

where dS is area element.

Let us make a substitution:

$$dr = \left|\frac{dr}{dT}\right| dT = \frac{dT}{\left|\frac{dT}{dr}\right|}$$

changing integration variable from r to T.

Then, it follows that

$$\int_V e^{\left(-\frac{\epsilon}{k_B T(\vec{\mathbf{r}})}\right)} \frac{n_p^2(\vec{\mathbf{r}}) dS dr}{\sqrt{T(\vec{\mathbf{r}})}} = \int_T \int_S e^{\left(-\frac{\epsilon}{k_B T(\vec{\mathbf{r}})}\right)} \frac{n_p^2(\vec{\mathbf{r}})}{\sqrt{T(\vec{\mathbf{r}})}\left|\frac{dT}{dr}\right|} dS\, dT =$$

$$= \int_T \frac{\xi(T)}{\sqrt{T(\vec{\mathbf{r}})}} \exp\left(-\frac{\epsilon}{k_B T(\vec{\mathbf{r}})}\right) dT,$$

where

$$\xi(T) = \int_{S_T} \frac{n_p^2(\vec{\mathbf{r}})}{\left|\frac{dT}{dr}\right|} dS$$

is the differential emission measure and S_T denotes spherical surface of constant temperature T, at radius r.

Things simplify further if the plasma density is also spherically symmetric i.e. $n_p(\vec{\mathbf{r}}) = n_p(r)$. Note the problems in the example sheet.

7.9 Isothermal surfaces

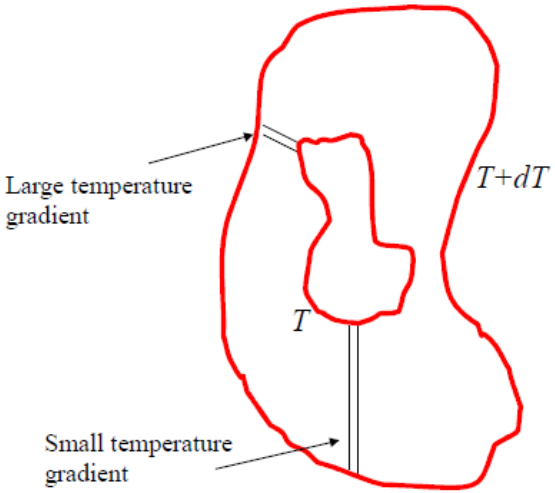

Figure 7.3: *Isothermal surfaces*

More generally $T = T(r, \theta, \varphi)$ but we can still change variables in the integral by identifying **isothermal surfaces** - i.e. surfaces of constant temperature (which will not in general be spherical).

The source emission measure is now defined in terms of the temperature gradient, ∇T

$$\xi(T) = \int_{S_T} \frac{n_p^2(\vec{\mathbf{r}})}{|\nabla T|} dS$$

but we will not consider any non-spherical cases here.

7.10 Examples of inhomogeneous plasma

The differential emissivity from non-uniformly heated plasma can be presented using $\xi(T)$, see Equation 7.4:

$$\frac{1}{\epsilon}\frac{dL}{d\epsilon} = \frac{dJ}{d\epsilon} = 2\sqrt{\frac{2}{\pi m}}\frac{Q_0 mc^2}{k^{1/2}\epsilon}\int_0^\infty \xi(T)\frac{1}{T^{1/2}}\exp\left(-\frac{\epsilon}{k_B T}\right)dT$$

A wide range of behaviour for $\xi(T)$ is possible:

- $\xi(T)$ smoothly varying in an extended gas cloud (e.g. solar corona, galaxy cluster Figure 7.4)
- $\xi(T)$ has a sharp change or discontinuous across a shock front (e.g. transition region in the solar atmosphere, supernova remnant, Figure 7.5)

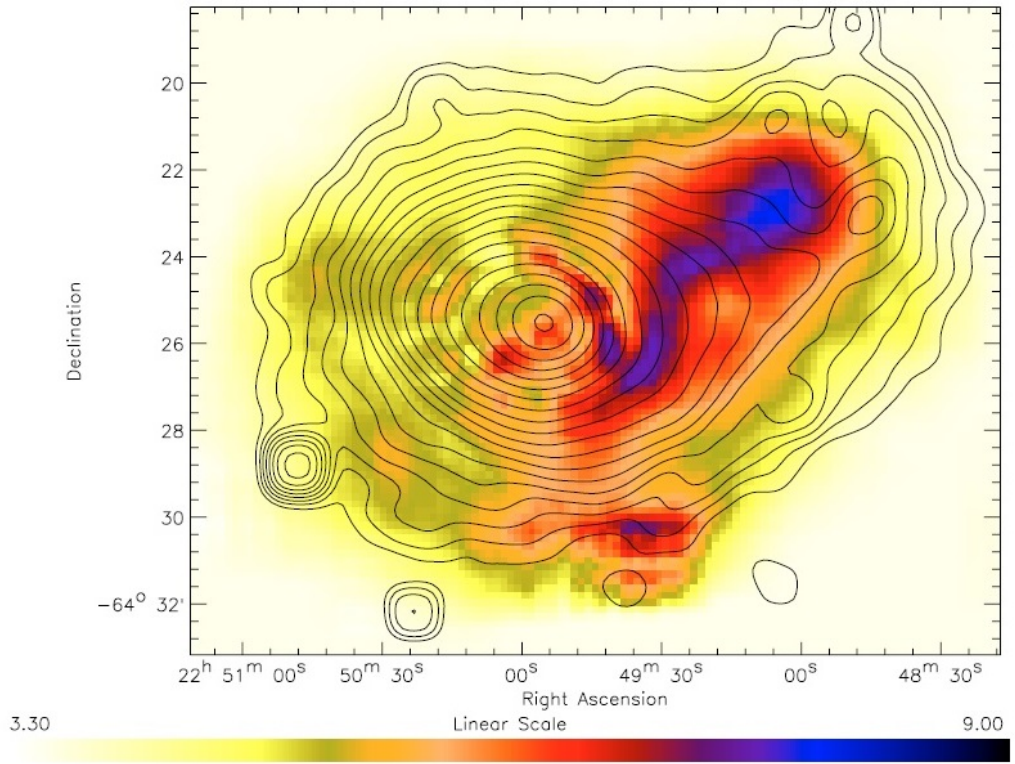

Figure 7.4: *Temperature structure of the galaxy cluster Abell 3921. From Belsole et al, 2005*

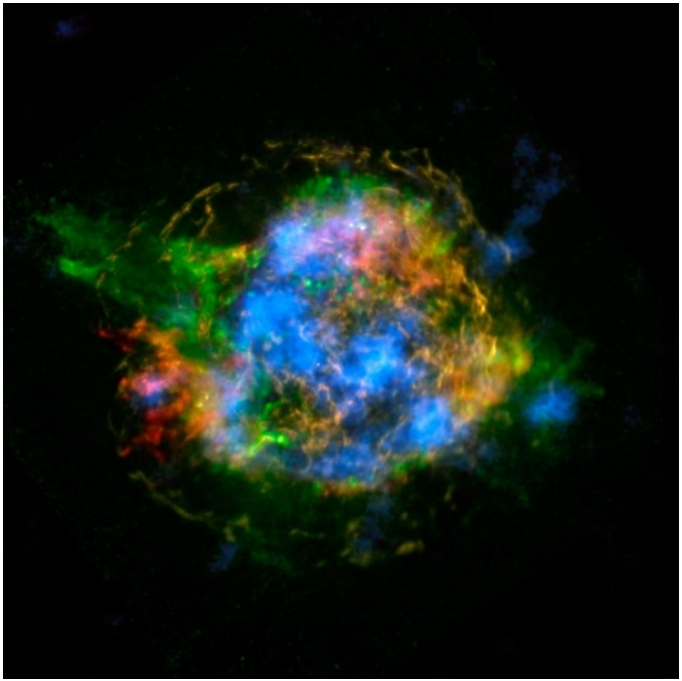

Figure 7.5: *Cassiopeia A Supernova Remnant: In this false-color image, NuSTAR data, which show high-energy X-rays from radioactive material, are colored blue. Lower-energy X-rays from non-radioactive material, imaged previously with NASA's Chandra X-ray Observatory, are shown in red, yellow and green from NuSTAR webpage*

8 Photon spectrum interpretation

LECTURE OUTLINE

- Ambiguity between thermal and non-thermal processes
- Electron energy spectrum from photon spectrum

8.1 Mimicking Non-thermal Processes

We saw earlier that, if the non-thermal differential electron flux distribution is a **power law**, then the differential photon luminosity is also a power law, with the same exponent.

If, instead, we have a **thermal plasma**, but not an **isothermal** plasma, then we can also obtain a power law photon spectrum - provided the source emission measure function has a power law dependence on temperature, i.e. [4]

$$\text{if} \quad \xi(T) \propto T^{-\alpha} \quad \text{then} \quad \frac{dL}{d\epsilon} \propto \epsilon^{-\beta}$$

with $\alpha \neq \beta$, but **there is ambiguity between thermal and non-thermal processes**.

[4] See problem sheet

8.2 Interpreting Energy Spectra

The fact that measurements of $dJ/d\epsilon$ and $dL/d\epsilon$ are not perfect, but are subject to **experimental errors**, raises some **important** numerical issues.

The problem is to determine, from $dJ/d\epsilon$:

- $\xi(T)$ for a **thermal** source
- $F(E)$ for a **non-thermal** source

Consider a non-thermal source, homogeneous plasma:

$$\frac{dJ}{d\epsilon} = \frac{Q_0 mc^2}{\epsilon} n_p V \int_{\epsilon}^{\infty} \frac{F(E)}{E} dE$$

The integral

$$\int_{\epsilon}^{\infty} \frac{F(E)}{E} dE$$

is a function of photon energy, ϵ. We define

$$G(\epsilon) = \int_{\epsilon}^{\infty} \frac{F(E)}{E} dE$$

It follows that

$$\frac{dJ}{d\epsilon} = \frac{Q_0 mc^2}{\epsilon} n_p V G(\epsilon)$$

Then

$$G(\epsilon) = \frac{1}{Q_0 mc^2 n_p V} \epsilon \frac{dJ}{d\epsilon}$$

Let us differentiate $G(\epsilon)$[5]

$$\frac{dG}{d\epsilon} = \frac{d}{d\epsilon}\int_{\epsilon}^{\infty} \frac{F(E)}{E} dE = -\left.\frac{F(E)}{E}\right|_{E=\epsilon}$$

then we can find

$$F(E) = -\left(\epsilon \frac{dG}{d\epsilon}\right)\Big|_{\epsilon=E} = -E\left.\frac{dG}{d\epsilon}\right|_{\epsilon=E}$$

and substituting expression for $G(\epsilon)$, we have

[5] If f(y) is a function that is continuous on our interval, then

$$\frac{d}{dx}\int_{a(x)}^{b(x)} f(y)dy = f(b(x))\frac{db}{dx} - f(a(x))\frac{da}{dx}$$

where $a(x)$ and $b(x)$ are functions of x.

$$F(E) = \frac{-E}{Q_0 mc^2 n_p V} \frac{d}{d\epsilon} \epsilon \frac{dJ}{d\epsilon}\bigg|_{\epsilon=E} = \\ = \frac{-E}{Q_0 mc^2 n_p V} \left[\frac{dJ}{d\epsilon} + \epsilon \frac{d}{d\epsilon} \left(\frac{dJ}{d\epsilon} \right) \right]\bigg|_{\epsilon=E} \qquad (8.1)$$

Since the solution (8.1) for $F(E)$ involves the **derivative** of the photon energy spectrum, $\frac{dJ}{d\epsilon}$, this means that small changes in the measured data for $\frac{dJ}{d\epsilon}$ can lead to large changes in the inferred $F(E)$. [6]

To solve the problem with large errors, we **need to apply regularization**. Extraction of electron spectrum from photon spectrum is a challenge, see e.g. Brown et al, 2006.

[6] This an example of an ill-posed inverse problem.

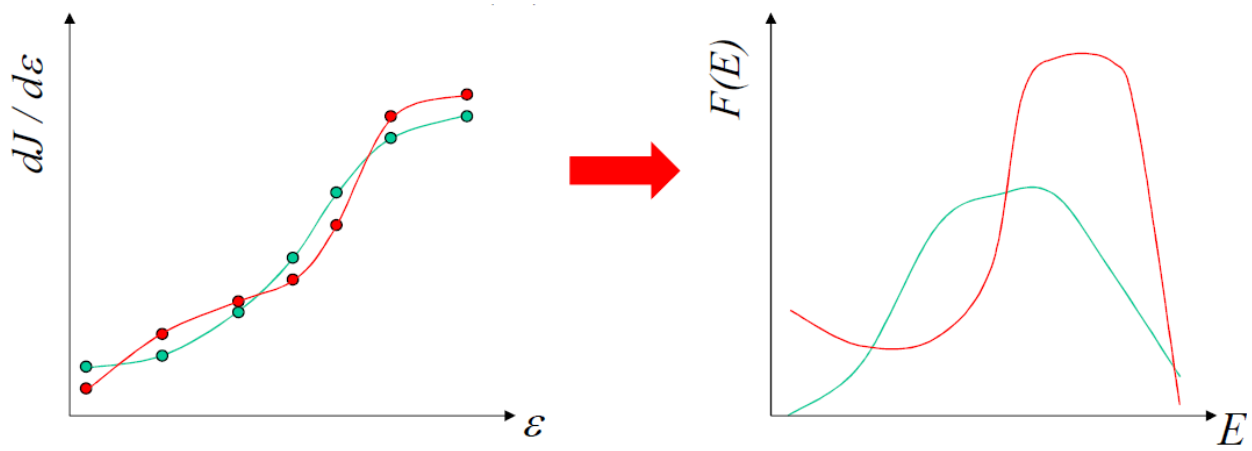

Figure 8.1: ***Left:*** *Two weakly different X-ray spectra* $dJ/d\varepsilon$. ***Right:*** *Two corresponding electron spectra* $F(E)$ *showing large differences after differentiation in Equation 8.1.*

8.3 Example: Hard X-ray spectrum of a solar flare

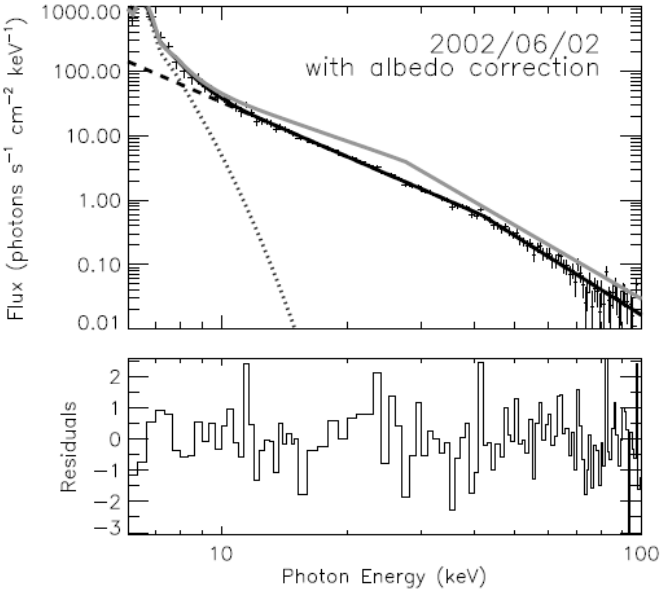

Figure 8.2: *Albedo-corrected RHESSI spectrum (crosses with error bars) at the hard X-ray peak of the solar flare on 2002-06-02 from Holman et al, 2011. The solid line shows the combined isothermal (dotted line) plus double power-law (dashed line) spectral fit. The spectral fit before albedo correction is over-laid (gray, solid line).*

8.4 Example: Derivative of a noisy data

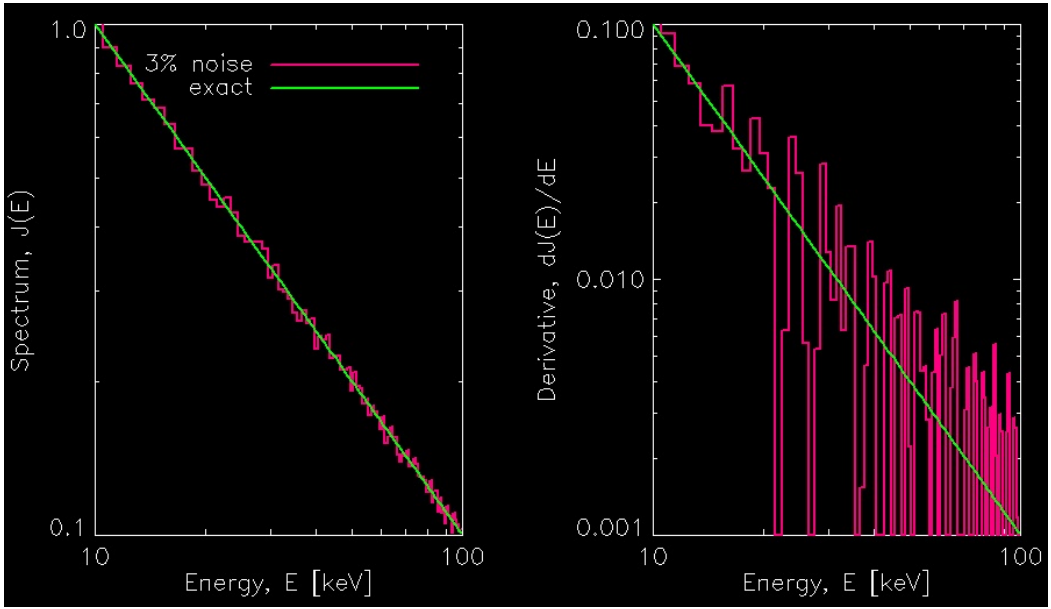

Figure 8.3: *A power-law spectrum $J(E) \propto 1/E$ (left panel) and the absolute value of the derivative $|dJ/dE| \propto 1/E^2$ (right panel); without and **with** 3% Gaussian noise added. See python 3.6 code online.*

8.5 Derivative as an inverse problem

Let us assume that we have a smooth function $J(E)$ over the interval $E_{01} \leq E \leq E_{02}$. We have a finite sample J_i of measured values of this function, obtained over some grid $E_{01} = E_0 < E_1 < ... < E_i < ... < E_n = E_{02}$ with mesh size ΔE. The noisy data set has an error

$$|J_i - J(E_i)| \leq \delta J \tag{8.2}$$

where δJ is an uncertainty of measurement.

We want to find the best smooth estimate of the derivative $J'(E)$ using the given data set $\forall\, E \in [E_{01}, E_{02}]$. The two point finite difference estimate is readily available with the following bound

$$\left|\frac{J_{i+1} - J_i}{\Delta E} - J'(E_i)\right| \leq O(\Delta E + \frac{\delta J}{\Delta E}), \tag{8.3}$$

where the first and second terms in the right hand side represent consistency and propagation errors respectively.

8.6 Thermal X-ray Emission Lines

Hot astrophysical plasmas in e.g. the Sun contain traces of heavier elements which are partially (often highly!) ionised.

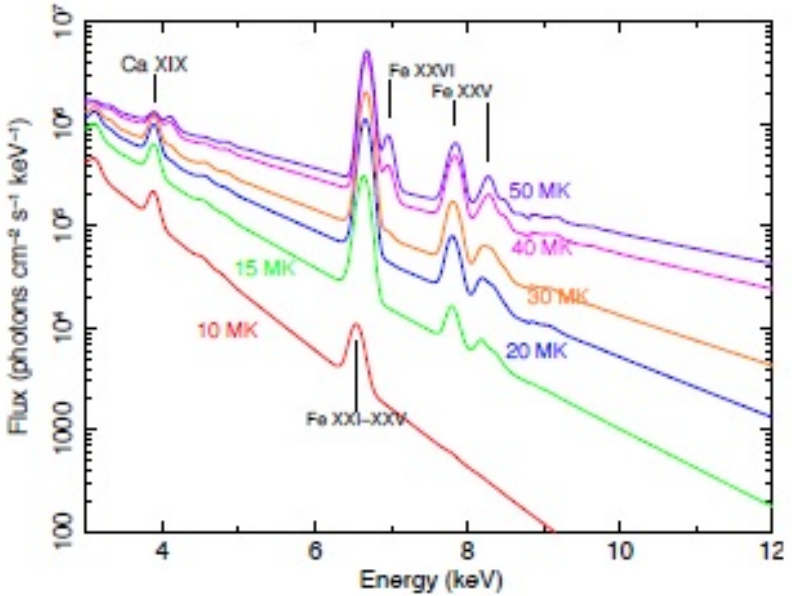

Figure 8.4: *Simulated X-ray spectra of solar flare plasma thermal emission for a range of plasma temperatures from 10 to 50 MK, from Skinner et al, 2013*

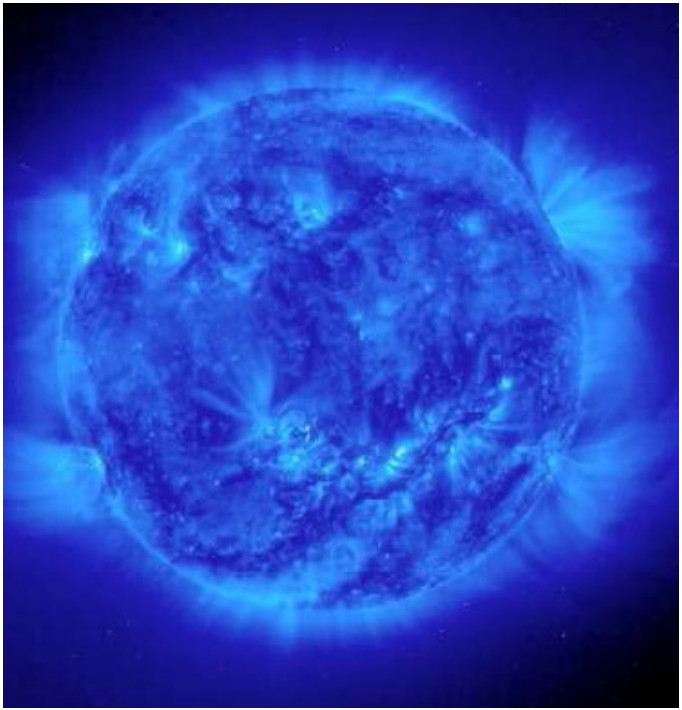

Figure 8.5: *The Sun at 171 Å chiefly emitted by Fe IX and X at million degrees K. Elements produce emission lines, superimposed on a thermal background (Fig 3.7). Such emission lines can be observed using* ***narrow filters****, sensitive to only a narrow range of X-ray energies (temperatures).*

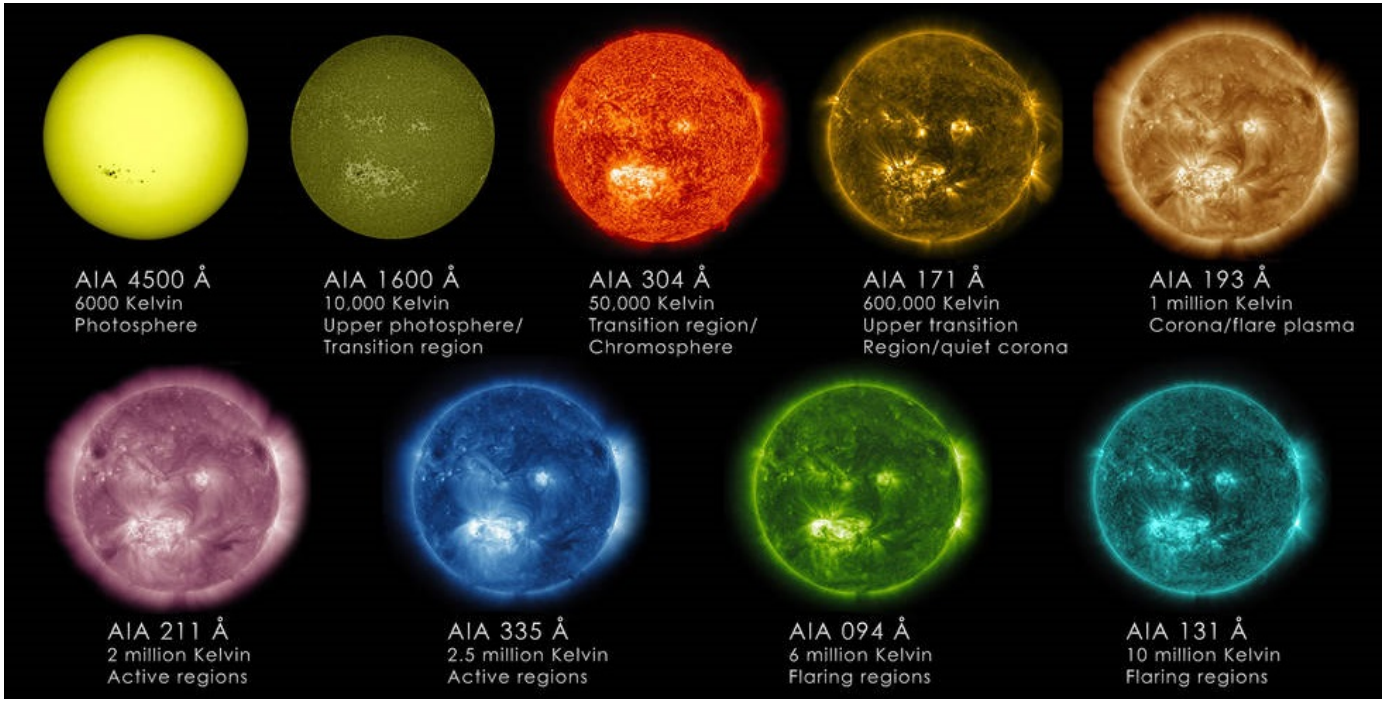

Figure 8.6: *Multi-temperature solar corona from SDO/AIA observations of multi-temperature corona.*

9 Inverse Compton Scattering

LECTURE OUTLINE

- Compton (inverse Compton) scattering
- Kinematics of the scattering (head-on collision)
- Energy gain due to the scattering
- Validity of approximations used

9.1 Thompson scattering and Compton scattering

The scattering of photons in media due to their interaction with electrons.

Thompson scattering (which we already discussed in Lecture 5) is the special case of **Compton scattering** in the limit of a low energy incoming photon - i.e. in the rest frame of the electron, the photon has incoming frequency ν, such that

$$h\nu \ll mc^2$$

In this low energy limit, the frequency ν', of the outgoing photon satisfies

$$\nu = \nu'$$

and the reaction cross-section is equal to the Thompson cross-section (see Section 5). **This is purely classical result.**

9.2 Compton Scattering

More generally (Compton, 1923, Klein & Nishina, 1929), we need to take into account :

1) **Modification of cross-section**

Thompson cross-section replaced by **Klein-Nishina** formula

$$Q_{KN} = Q_T \left[1 - 2\frac{h\nu}{mc^2} + \frac{25}{6}\left(\frac{h\nu}{mc^2}\right)^2 - \ldots \right]$$

2) **Electron recoils**, and absorbs some of the photon's energy , so that

$$\nu > \nu'$$

e.g. energy loss by a photon.

9.3 Inverse Compton Scattering

A low energy photon collides with a relativistic electron and gains energy at the expense of the electron (e.g. radio photons might be boosted to X-ray energies). So for **Inverse Compton scattering** we want

$$E' \ll E, \quad \nu' \gg \nu$$

In most astrophysical situations it is still OK to assume that, in the rest frame of the electron, the energy of the photon before collision is much less than the rest mass energy of the electron i.e.:

$$h\nu \ll mc^2$$

This means that we do not need to use the Klein-Nishina formula, but we can **assume**

$$Q_{IC} \approx Q_T = \frac{8}{3}\pi r_e^2$$

9.4 Kinematics (head-on collision)

To study the kinematics of inverse Compton scattering, we consider first the case of a **head-on collision**.

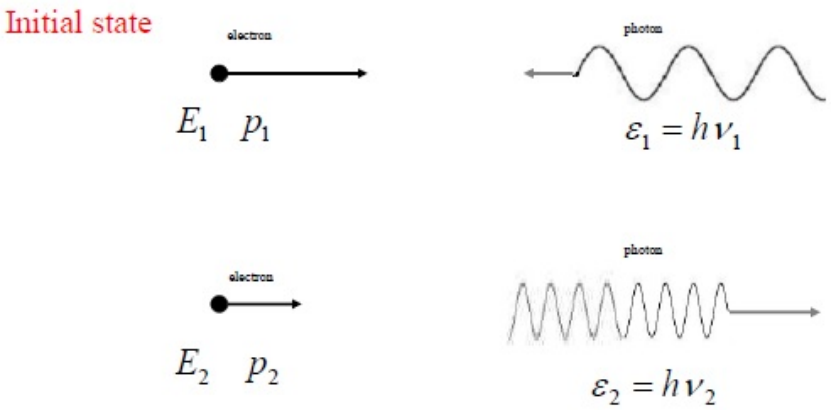

Figure 9.1: *Photon of energy ϵ, scattered through* 180^o *by a relativistic electron of initial energy* E_1.

Recall from special relativity, energy and momentum together make up the

4-vector, 4-momentum and **Lorentz factor** is $\gamma = \frac{1}{\sqrt{1-v^2/c^2}}$

For the **photon**:

$$\text{energy:} \quad \epsilon = h\nu$$

$$\text{momentum:} \quad p = \frac{\epsilon}{c} = \frac{h\nu}{c}$$

For **electron**:

$$\text{energy:} \quad E = \gamma mc^2$$

$$\text{momentum:} \quad p = \gamma mv$$

Let us recall the useful relation, for the electron

$$E^2 = p^2c^2 + m^2c^4$$

hence

$$p^2 = \frac{E^2}{c^2} - m^2c^2 = \gamma^2 m^2 c^2 - m^2 c^2 = (\gamma^2 - 1)m^2c^2$$

$$\Longrightarrow \quad p = mc\sqrt{\gamma^2 - 1}$$

By the conservation of energy, we have

$$E_1 + \epsilon_1 = E_2 + \epsilon_2$$

$$E_1 - E_2 = \Delta E = \epsilon_2 - \epsilon_1 \tag{9.1}$$

and conservation of momentum:

$$p_1 - \frac{\epsilon_1}{c} = p_2 + \frac{\epsilon_2}{c} \tag{9.2}$$

We want to express ϵ_2 (**final photon energy**) in terms of ϵ_1 and E_1, i.e. we want to eliminate E_2.

We introduce the dimensionless energy variable for the photon

$$\rho = \frac{\epsilon}{mc^2}$$

analogous to

$$\gamma = \frac{E}{mc^2}$$

Equations (9.1, 9.2) give

$$\gamma_1 - \gamma_2 = \rho_2 - \rho_1 = \Delta\rho \tag{9.3}$$

$$\sqrt{\gamma_1^2 - 1} - \rho_1 = \sqrt{\gamma_2^2 - 1} + \rho_2 \tag{9.4}$$

Thus

$$\gamma_2 = \gamma_1 - \Delta\rho$$

$$\sqrt{\gamma_1^2 - 1} - \sqrt{\gamma_2^2 - 1} = \rho_1 + \rho_2 = 2\rho_1 + \Delta\rho$$

Substituting for γ_2:

$$\sqrt{\gamma_1^2 - 1} - \sqrt{(\gamma_1 - \Delta\rho)^2 - 1} = 2\rho_1 + \Delta\rho$$

$$\Longrightarrow \quad (\gamma_1 - \Delta\rho)^2 - 1 = \left[\sqrt{\gamma_1^2 - 1} - (2\rho_1 + \Delta\rho)\right]^2$$

simplifying, one obtains

$$\Longrightarrow \quad \Delta\rho\left[\gamma_1 + 2\rho_1 - \sqrt{\gamma_1^2 - 1}\right] = 2\rho_1\left[\sqrt{\gamma_1^2 - 1} - \rho_1\right]$$

$$\Delta\rho = \frac{2\rho_1\left[\sqrt{\gamma_1^2 - 1} - \rho_1\right]}{\left[\gamma_1 + 2\rho_1 - \sqrt{\gamma_1^2 - 1}\right]} \tag{9.5}$$

We can further simplify this formula by noting that, for astrophysical examples

of inverse Compton scattering, we have:

$$\textbf{Low energy incoming photons:} \quad \rho_1 \ll 1$$
$$\textbf{High energy incoming electrons:} \quad \gamma_1 \gg 1$$

so we have from Equation (9.5)

$$\Delta\rho = \frac{2\rho_1\left[\sqrt{\gamma_1^2-1}-\rho_1\right]}{\left[\gamma_1+2\rho_1-\sqrt{\gamma_1^2-1}\right]} = \frac{2\rho_1\gamma_1\left[\sqrt{1-1/\gamma_1^2}-\rho_1/\gamma_1\right]}{\gamma_1\left[1+2\rho_1/\gamma_1-\sqrt{1-1/\gamma_1^2}\right]}$$

Let us retain first order terms in $1/\gamma_1$, and using that $(1+x)^n \simeq 1+nx$, we can derive

$$\Delta\rho = \frac{2\rho_1\left[1-1/2\gamma_1^2-\rho_1/\gamma_1\right]}{\left[1+2\rho_1/\gamma_1-1+1/2\gamma_1^2\right]} \simeq \frac{2\rho_1\gamma_1^2}{[2\rho_1\gamma_1+1/2]} = \frac{4\rho_1\gamma_1^2}{[4\rho_1\gamma_1+1]} \qquad (9.6)$$

Equation 9.6 can be further simplified. However, since we assumed $\gamma_1 \gg 1$, and $\rho_1 \ll 1$, the value $\gamma_1\rho_1$ is undefined, i.e. $\gamma_1\rho_1 \gg 1$ or $\gamma_1\rho_1 \ll 1$

Let us first consider the case $\gamma_1\rho_1 \gg 1$ in 9.6:

$$\Delta\rho \simeq \frac{4\rho_1\gamma_1^2}{[4\rho_1\gamma_1 + 1]} \simeq \gamma_1 \tag{9.7}$$

Equation 9.7 is approximation saying that photon gains all the energy of the incoming electron.

However, even larger relative boost can be achieved if $\rho_1\gamma_1 \ll 1$.

Let us now consider the case $\rho_1\gamma_1 \ll 1$ in Equation (9.6), so we can write:

$$\Delta\rho \simeq \rho_2 \simeq 4\rho_1\gamma_1^2 \tag{9.8}$$

since $\Delta\rho = \rho_2 - \rho_1 \simeq \rho_2$.

Note that a head-on collision gives the maximum energy transfer to the outgoing photon.

Averaging over all scattering directions gives approximately:

$$\langle \rho_2 \rangle \simeq \frac{4}{3}\gamma_1^2 \rho_1 \tag{9.9}$$

when averaged over all angles.

9.5 Example I

Let us consider head-on collision between an **optical photon** $\epsilon_1 = 1$ eV and a cosmic ray electron.

Note that $\rho_1 = \epsilon_1/mc^2 = 10^{-3}/511 \simeq 2 \times 10^{-6}$.

	X-rays	Gamma-rays	
Scattered photon, ε_2	1 keV	1 MeV	1 GeV
$\frac{\rho_2}{\rho_1} = \frac{\varepsilon_2}{\varepsilon_1} = 4\gamma_1^2$	10^3	10^6	10^9
γ_1	16	500	16000
Electron energy, $E_1 = \gamma_1 m_e c^2$	8 MeV	250 MeV	8 GeV
$\rho_1 \gamma_1$	3.2×10^{-5}	10^{-3}	3.2×10^{-2}

9.6 Example II

For a **CMBR photon** $\epsilon_1 = 10^{-3}$ eV and a cosmic ray electron. Note that $\rho_1 = \epsilon_1/mc^2 = 10^{-6}/511 \simeq 2 \times 10^{-9}$.

	X-rays	← Gamma-rays →	
Scattered photon, ε_2	1 keV	1 MeV	1 GeV
$\frac{\rho_2}{\rho_1} = \frac{\varepsilon_2}{\varepsilon_1} = 4\gamma_1^2$	10^6	10^9	10^{12}
γ_1	500	16000	500000
Electron energy, $E_1 = \gamma_1 m_e c^2$	250 MeV	8 GeV	250 GeV
$\rho_1 \gamma_1$	10^{-6}	3.2×10^{-5}	10^{-3}

9.7 Validity of approximations

Two examples show that in two cases:

- Head-on collision between a CMBR photon and a cosmic ray electron
- Head-on collision between an optical photon and a cosmic ray electron

In all cases we considered, $\rho_1\gamma_1 \ll 1$, as we assumed in deriving the expression for ρ_2.

10 Inverse Compton Luminosity and Spectrum

LECTURE OUTLINE

- Inverse Compton luminosity
- Compton scattering cross-section
- Inverse Compton luminosity spectrum

10.1 Inverse Compton Luminosity

Consider a homogeneous volume, V, filled with electrons all of energy $E = \gamma mc^2$ and number density n_e, and photons all of energy $\epsilon = h\nu$ and number density n_ν

Total emissivity from this volume is given by (see Equation 4.2):

$$J = N_T F Q$$

We regard the photons as the target particles, hit by a beam of highly relativistic electrons. Thus:

$$N_T = n_\nu V \quad \text{and} \quad F = n_e v \simeq n_e c$$

so that

$$J = n_\nu V n_e c Q_{IC} \tag{10.1}$$

From previous section, average energy of a scattered photon,

$$\langle \epsilon_2 \rangle \simeq \frac{4}{3}\gamma^2 h\nu$$

Thus, average source luminosity from Equation (10.1)

$$L = J\langle \epsilon_2 \rangle = n_\nu V n_e c Q_{IC} \frac{4}{3}\gamma^2 h\nu$$

We can re-write this as follows:

$$L_{IC} = \frac{4}{3} c\gamma^2 \underbrace{N_e}_{=n_e V} Q_{IC} \underbrace{U_\nu}_{=n_\nu h\nu} , \quad \text{[W]} \qquad (10.2)$$

where U_ν is the radiation energy density.

Hence, the **average IC power emitted from N_e electrons of energy γmc^2**

$$\left(\frac{dE}{dt}\right)_{IC} = L_{IC} = \frac{4}{3} Q_{IC} c N_e \gamma^2 U_\nu \quad \text{[W]} \qquad (10.3)$$

which is also the energy loss rate of the electrons.

10.2 Lifetime of an electron and IC losses

Power emitted by a single electron

$$L_{IC} = \frac{4}{3} Q_{IC} c \gamma^2 U_\nu$$

Timescale for an electron to lose its energy

$$\tau_{IC} \approx \frac{E}{\frac{dE}{dt}} = \frac{\gamma m c^2}{\frac{32}{9} \pi r_e^2 c \gamma^2 U_\nu} = \frac{9mc}{32\pi r_e^2} \frac{1}{\gamma U_\nu}$$

Let us consider e.g., CMBR photons $T \simeq 2.7$ K. From **black body radiation energy density** (see Equation 3.6 and description in Section 3.10)

$$U_\nu = aT^4 \simeq 4 \times 10^{-14}, \quad [\text{J m}^{-3}]$$

Timescale for an electron to lose its energy in CMBR background

$$\tau_{IC} \approx \frac{9mc}{32\pi r_e^2} \frac{1}{\gamma U_\nu} \simeq \frac{2 \times 10^{12}}{\gamma} \quad [\text{ years}]$$

For, e.g., 1 GeV electron

$$\gamma = \frac{E}{mc^2} \simeq 2 \times 10^3$$

we have $\tau_{IC} \simeq 10^9$ years.

10.3 IC spectrum

In a real situation the electrons and photons would have a distribution of initial energies, on which the **Inverse Compton cross-section**, Q_{IC} would depend - i.e. for an IC photon of outgoing energy $\epsilon = h\nu$ we have

$$\frac{dQ_{IC}}{d\epsilon} = \frac{dQ_{IC}}{d\epsilon}(h\nu_0, E)$$

where $h\nu_0$ is the energy of incoming photon, E is the energy of incoming electron. Further

$$\frac{dJ_{IC}}{d\epsilon} = c \int\int\int \frac{dn_e}{dE}\frac{dn_\nu}{d\nu_0}\frac{dQ_{IC}}{d\epsilon} d\nu_0 dE dV$$

We can define the electron energy before collision via $\gamma = E/mc^2$, so that we can also write

$$\frac{dJ_{IC}}{d\epsilon} = c \int\int\int \frac{dn_e}{d\gamma}\frac{dn_\nu}{d\nu_0}\frac{dQ_{IC}}{d\epsilon} d\nu_0 d\gamma dV$$

and

$$\frac{dL_{IC}}{d\epsilon} = c\epsilon \int\int\int \frac{dn_e}{d\gamma}\frac{dn_\nu}{d\nu_0}\frac{dQ_{IC}}{d\epsilon} d\nu_0 d\gamma dV$$

We can simplify this integral by make **the assumption that all emitted photons gain the average amount of energy** i.e.

$$\frac{dQ_{IC}}{d\epsilon} = 0 \quad \text{unless} \quad \epsilon = \frac{4}{3}\gamma^2 h\nu_0$$

we can write this as

$$\frac{dQ_{IC}}{d\epsilon} = \frac{8}{3}\pi r_e^2 \delta\left(\frac{4}{3}\gamma^2 h\nu_0 - \epsilon\right) = Q_T \delta\left(\frac{4}{3}\gamma^2 h\nu_0 - \epsilon\right) \qquad (10.4)$$

where $\delta(x)$ is **Dirac delta function**. Noting that Dirac delta function has the following properties:

$$\delta(x - x_0) = 0 \quad \text{if} \quad x \neq x_0$$

$$\int_{-\infty}^{\infty} \delta(x - x_0)dx = 1 \quad \text{and} \quad \int_{-\infty}^{\infty} f(x)\delta(x - x_0)dx = f(x_0)$$

Changing variables from γ to $x = 4/3\gamma^2 h\nu_0$ at fixed ν_0, we have:

$$\frac{dL_{IC}}{d\epsilon} = c\epsilon \int\int\int \frac{dn_e}{d\gamma}\frac{dn_\nu}{d\nu_0} Q_T \delta(x - \epsilon)d\nu_0 \frac{3}{8\gamma h\nu_0} dx dV$$

Integrating over the electron energy x

$$\frac{dL_{IC}}{d\epsilon} = c\epsilon Q_T \int\int \left(\frac{dn_e}{d\gamma}\frac{3}{8\gamma h\nu_0}\right)\Bigg|_{x=\epsilon} \frac{dn_\nu}{d\nu_0} d\nu_0 dV$$

Substituting back $\epsilon = x = \frac{4}{3}\gamma^2 h\nu_0$ and simplifying, we find **luminosity spectrum of Inverse Compton emission** for arbitrary electron and photon spectra

The luminosity differential in energy

$$\frac{dL_{IC}}{d\epsilon} = cQ_T \int\int \left(\frac{\gamma}{2}\frac{dn_e}{d\gamma}\right)\Big|_{\gamma=\sqrt{\frac{3\epsilon}{4h\nu_0}}} \frac{dn_\nu}{d\nu_0} d\nu_0 dV, \quad [\text{W keV}^{-1}] \quad (10.5)$$

depends on electron spectrum.

Now we need to assume the spectrum of incoming electrons.

10.4 Power-law spectrum of electrons

Suppose we have a power-law electron spectrum independent of position i.e.

$$\frac{dn_e}{d\gamma} = K\gamma^{-\alpha} \tag{10.6}$$

Then

$$\left(\frac{\gamma}{2}\frac{dn_e}{d\gamma}\right)\Big|_{\gamma=\sqrt{\frac{3\epsilon}{4h\nu_0}}} = \frac{K}{2}\gamma^{-\alpha+1} = \frac{K}{2}\left(\frac{3\epsilon}{4h\nu_0}\right)^{\frac{1-\alpha}{2}}$$

so luminosity differential in energy

$$\frac{dL_{IC}}{d\epsilon} = c\frac{8}{3}\pi r_e^2\frac{K}{2}\left(\frac{3}{4h}\right)^{\frac{1-\alpha}{2}}\epsilon^{\frac{1-\alpha}{2}}\int\int \nu_0^{\frac{\alpha-1}{2}}\frac{dn_\nu}{d\nu_0}d\nu_0 dV, \quad [\text{ W keV}^{-1}] \tag{10.7}$$

i.e. if we neglect the constants.

The proportionality becomes

$$\frac{dL_{IC}}{d\epsilon} \propto \epsilon^{-\beta}, \quad \text{where} \quad \beta = \frac{\alpha - 1}{2} \tag{10.8}$$

So, again, we find that a **power-law distribution of electron energies** gives rise to a **power law photon spectrum**, but with a **different** power law index.

10.5 Summary of power-law spectra

X-ray mechanism	Electron distribution	Photon index
Non-thermal Bremsstrahlung	$F(E) \propto E^{-\delta}$	$\frac{dL}{d\epsilon} \propto \epsilon^{-\delta}$
Thermal inhomogeneous plasma	$\xi \propto T^{-\alpha}$	$\frac{dL}{d\epsilon} \propto \epsilon^{-\beta}$
Inverse Compton scattering	$\frac{dn_e}{d\gamma} \propto \gamma^{-\alpha}$	$\frac{dL}{d\epsilon} \propto \epsilon^{-\frac{(\alpha-1)}{2}}$

Note spectrum for **synchrotron radiation** in the next section.

11 Synchrotron radiation: luminosity and spectrum

LECTURE OUTLINE

- Synchrotron radiation luminosity
- Synchrotron radiation cross-section
- Synchrotron radiation luminosity spectrum

11.1 Cyclotron radiation

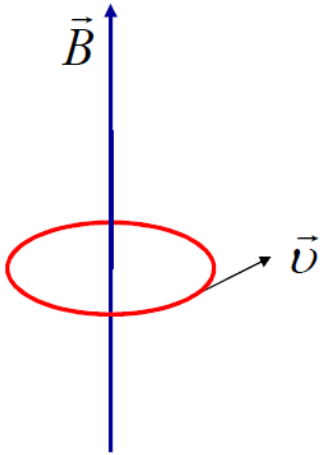

Figure 11.1: *Electron gyrating in* $\vec{\mathbf{B}}$ *field*

Consider a non-relativistic electron, with $v \ll c$, following a circular orbit or radius, r, 'around' a field line of a uniform magnetic field, $\vec{\mathbf{B}}$.

Lorentz force gives circular motion (Figure 11.1)

$$evB = \frac{mv^2}{r} \quad \Longrightarrow \quad \omega_L = \frac{v}{r} = \frac{eB}{m}$$

where ω_L is **Larmor angular frequency**. Electron emits **cyclotron radiation** at the **Larmor frequency** ν_L

$$\nu_L = \frac{\omega_L}{2\pi} = \frac{eB}{2\pi m} \tag{11.1}$$

Any constant velocity component parallel to the magnetic field does not lead to radiation (no change in acceleration, recall Equation 5.2).

11.2 Cyclotron line features

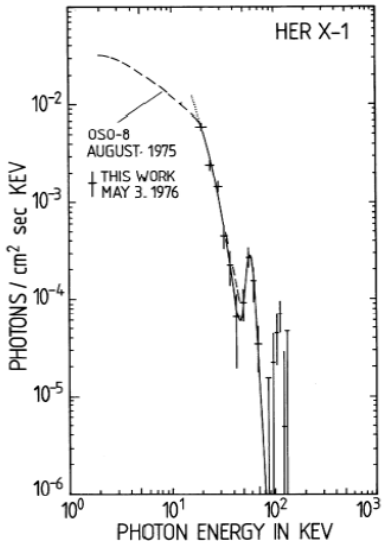

Figure 11.2: *Hercules X-1 X-ray spectrum from Trumper et al, 1978*

Cyclotron line has energy:

$$\epsilon = h\nu_L = \frac{heB}{2\pi m} \simeq 10^{-7}B, \quad [\text{ keV Tesla}^{-1}]$$

Cyclotron lines are observed in X-ray binaries due to resonant scattering of the line of sight X-ray photons against electrons embedded in magnetic fields.

For e.g. Her X-1 (X-ray binary) has such feature near 37 keV, (discovered by Trumper et al, 1978 see also Furst et al, 2013) so can **diagnose magnetic field:**

$$B \simeq 3.7 \times 10^8, \quad [\text{ Tesla}]$$

Note that the strong magnetic fields are expected near to a neutron star.

11.3 Synchrotron Radiation

Consider now a highly relativistic electron $v \longrightarrow c$, and $\gamma \gg 1$.

Radiation is known as **synchrotron** and is strongly **Doppler shifted** and forward beamed due to relativistic aberration (Figure 11.3).

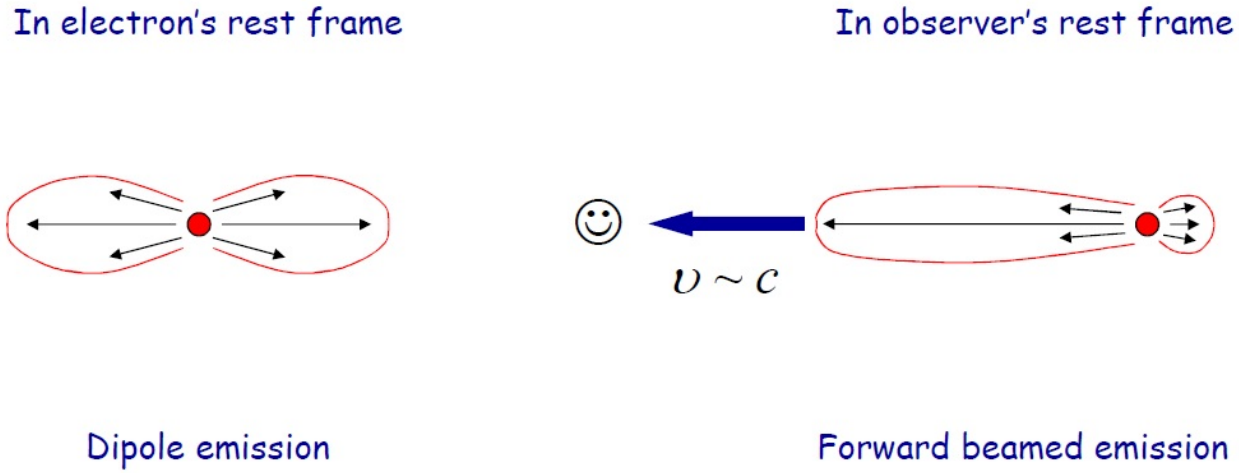

Figure 11.3: *Cartoon showing relativistic beaming of synchrotron radiation*

11.4 Synchrotron frequency and single electron spectrum

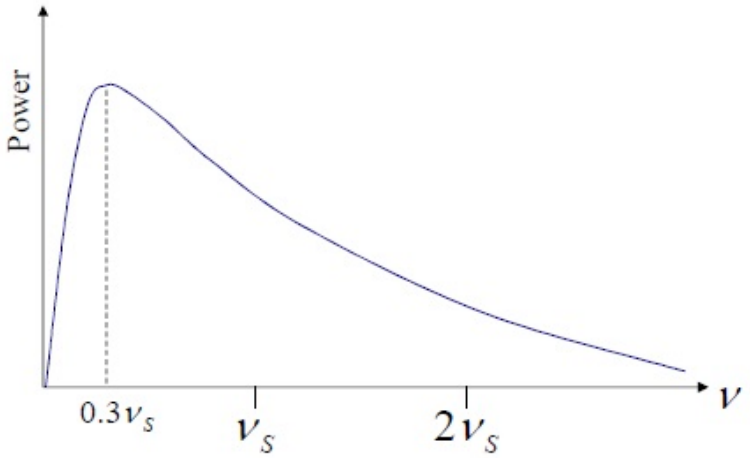

Figure 11.4: *Synchrotron spectrum of a single electron*

Typical frequency of synchrotron radiation is

$$\nu_s = \frac{3}{2}\gamma^2\nu_L = \frac{3}{2}\gamma^2\left(\frac{eB}{2\pi m}\right) \tag{11.2}$$

Synchrotron radiation is emitted over a wide range of frequencies (Figure 11.4).

Peak occurs at $\sim 0.3\nu_s$, but **average** frequency value $\langle\nu\rangle \simeq \nu_s$.

At low frequencies, $\nu \ll \nu_s$, the spectrum grows $\propto \nu^{1/3}$ (Figure 11.4).

11.5 Synchrotron luminosity

We can estimate the power radiated by a single electron using Equation 5.2:

$$P = \frac{e^2 \dot{v}^2}{6\pi\epsilon_0 c^3}$$

where the acceleration $\dot{v}$ can be determined by transforming to the electron's rest frame, in which electric field is:

$$\overrightarrow{\mathbf{E}'} = \gamma \vec{\mathbf{v}} \times \vec{\mathbf{B}}$$

From Newton's 2nd law

$$\frac{d\vec{\mathbf{v}}'}{dt'} = \frac{e}{m}\overrightarrow{\mathbf{E}'} = \frac{e\gamma}{m}\vec{\mathbf{v}} \times \vec{\mathbf{B}}$$

We can estimate the power radiated by a single electron is

$$\left(\frac{dE'}{dt'}\right)_S = \frac{e^2 \dot{v}'^2}{6\pi\epsilon_0 c^3} = \frac{e^2}{6\pi\epsilon_0 c^3}\left(\frac{ev\gamma B \sin(\theta)}{m}\right)^2 \tag{11.3}$$

where dE'/dt' is the power in electron rest's frame. But the power is an **Lorentz invariant**, e.g.

$$\frac{dE'}{dt'} = \frac{dE}{dt}$$

Hence the **observed power** radiated per electron is also given by the formula 11.3.

If $\vec{\mathbf{v}}$ is randomly oriented in 3-D, then $\langle \sin^2(\theta) \rangle = \frac{2}{3}$.

Also, the magnetic energy density is defined to be

$$U_B = \frac{B^2}{2\mu_0}$$

where μ_0 is permeability constant. Recalling Thomson cross-section (Equation 5.4)

$$Q_T = \frac{8\pi}{3}\left(\frac{e^2}{4\pi\epsilon_0 mc^2}\right)^2 = \frac{8\pi}{3} r_e^2$$

The power emitted by an electron (Equation 11.3) can be re-written:

$$\left(\frac{dE}{dt}\right)_S = \frac{e^2}{6\pi\epsilon_0 c^3}\frac{2}{3}\left(\frac{ev\gamma B}{m}\right)^2 = \frac{4}{3}Q_T c\gamma^2 U_B \qquad (11.4)$$

where we took $v = c$ and $\mu_0\epsilon_0 = 1/c^2$.

If we compare this formula (Equation 11.4) with our result for the Inverse Compton luminosity (Equation 10.3), one finds:

$$\frac{\left(\frac{dE}{dt}\right)_{IC}}{\left(\frac{dE}{dt}\right)_S} = \frac{U_\nu}{U_B} \qquad (11.5)$$

The ratio of Inverse Compton and Synchrotron luminosity from a source is given by the ratio of its radiation to magnetic energy density.

11.6 Synchrotron radiation from electron distribution

For a homogeneous volume, V, of uniform magnetic field, $\vec{\mathbf{B}}$, containing N_e electrons - all of energy $E = \gamma mc^2$ then (**as for the Inverse Compton case**) the total luminosity for N_e electrons is given by

$$L_S = \frac{4}{3} Q_T c N_e \gamma^2 U_B \quad [\text{W}] \tag{11.6}$$

As we considered in the Inverse Compton case, in a real situation the electrons would have a **distribution of energies**, and their number density would be a function of position. We need to take this into account when we calculate the synchrotron spectrum - i.e. the luminosity as a function of photon energy. Thus, **synchrotron luminosity spectrum** is

$$\frac{dL_S}{d\epsilon} = \int \int \frac{4}{3} c \gamma^2 \frac{dn_e}{d\gamma} U_B \frac{dQ_S}{d\epsilon} d\gamma dV \tag{11.7}$$

11.7 Synchrotron luminosity spectrum

To simplify matters, we make a similar approximation as in the **Inverse Compton case** (see Lecture 9): we assume that synchrotron emission only occurs at the mean synchroton frequency

$$\nu_s = \frac{3}{2}\gamma^2 \nu_L$$

and **all synchrotron photons** have energy:

$$\epsilon = h\nu_s = \frac{3}{2}\gamma^2 h\nu_L$$

This means that we assume the **synchrotron differential cross-section** takes the form:

$$\frac{dQ_S}{d\epsilon} = \frac{8}{3}\pi r_e^2 \delta\left(\frac{3}{2}\gamma^2 h\nu_L - \epsilon\right) \tag{11.8}$$

Hence, we can write the differential synchrotron spectrum as

$$\frac{dL_S}{d\epsilon} = \frac{4}{3}c \int\int \gamma^2 \frac{dn_e}{d\gamma} U_B \frac{8}{3}\pi r_e^2 \delta\left(\frac{3}{2}\gamma^2 h\nu_L - \epsilon\right) d\gamma dV$$

and integrating over γ, one finds [7]

the differential luminocity

$$\frac{dL_S}{d\epsilon} = \frac{4}{3} c Q_T \int \left(\frac{\gamma}{3h\nu_L} \frac{dn_e}{d\gamma} \right) \Big|_{\gamma = \sqrt{\frac{2\epsilon}{3h\nu_L}}} U_B dV \qquad (11.9)$$

Note the similarity to IC expression.

[7] Here one can use another property of Dirac delta function

$$\delta(f(x)) = \frac{1}{\texttt{f'(a)}} \delta(x - a),$$

where a is the root of $f(x)$ i.e. $f(a) = 0$.

11.8 Radiation from a power-law electron spectrum

Suppose we have a power-law electron spectrum independent of position i.e.

$$\frac{dn_e}{d\gamma} = K\gamma^{-\alpha}, \qquad \alpha > 0$$

Then assuming uniform distribution of electrons and uniform $\vec{\mathbf{B}}$:

$$\frac{dL_S}{d\epsilon} = \frac{4}{3} c Q_T \left(\frac{\gamma}{3h\nu_L} K\gamma^{-\alpha} \right) \Bigg|_{\gamma=\sqrt{\frac{2\epsilon}{3h\nu_L}}} \int U_B dV \tag{11.10}$$

or

$$\frac{dL_S}{d\epsilon} \propto \epsilon^{-\frac{\alpha-1}{2}}$$

which is the same result as for Inverse Compton Scattering.

11.9 Typical energies of synchrotron electrons and photons

We saw previously that, for extremely high magnetic fields (e.g. near to a pulsar), we can obtain X-ray cyclotron emission/absorption:

$$\epsilon = h\nu_L = \frac{heB}{2\pi m} \simeq 10^{-7}B \quad \text{[keV/Tesla]}$$

since $\nu_s = 3/2\gamma^2\nu_L$ we could in principle achieve X-ray synchrotron energies for more modest magnetic fields, provided γ is large enough.

For e.g. the Solar corona, fields of about **10-100 Gauss** [8] have been measured. Thus to observe X-ray synchrotron emission, with e.g. 10 keV, from the corona would in this case require

$$\frac{3}{2}\gamma^2 10^{-7}10^{-2} = 10$$

[8] Note that 1 Gauss $=10^{-4}$ Tesla

hence

$$\gamma^2 \simeq 10^{10} \quad \Longrightarrow v = 0.99999999995c$$

so v should be very close to c!

Suppose instead we take a more modest $v = 0.5c$

$$\gamma^2 = (1 - 0.25)^{-1} = \frac{4}{3}$$

$$\epsilon = 1.5\gamma^2 h\nu_L \simeq 2 \times 10^{-7} B \quad \text{[keV/Tesla]}$$

Thus for $B = 10^{-2}$ Tesla=100 Gauss, $\epsilon = 2 \times 10^{-6}$ eV or

$$\nu_L = \frac{2 \times 10^{-6} \times 1.6 \times 10^{-19}}{6.63 \times 10^{-34}} \simeq 480 \quad \text{[MHz]}$$

This is in the **radio part** of the E-M spectrum. Indeed, **gyro-synchrotron emission** peaking near ~ 10 GHz is often observed during solar flares (e.g. Figure 11.5), indicating mildly relativistic particles 0.1-1 MeV.

11.10 Solar energetic particles and gyro-synchrotron emission

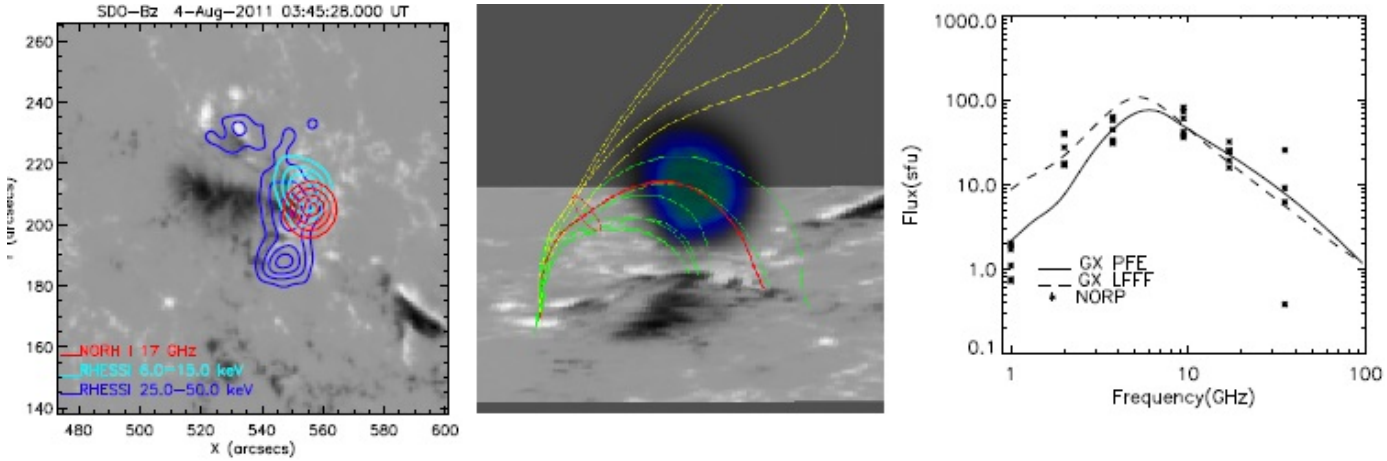

Figure 11.5: *Simulations (centre) of the spectrum (right) and the images (left) of radio emission provides strong evidence that the emission mechanism is (gyro-) synchrotron radiation - due to the acceleration of charged particles in the Sun' s magnetic field. From Nita et al, 2015*